Mach-Zehnder interferometry of fractional quantum Hall edge states

Ivan P. Levkivskyi,[1,2] Alexey Boyarsky,[3,4] Jürg Fröhlich,[3] and Eugene V. Sukhorukov[1]

[1]*Département de Physique Théorique, Université de Genève, CH-1211 Genève 4, Switzerland*
[2]*Department of Physics, Kyiv National University, 03022 Kyiv, Ukraine*
[3]*Institute of Theoretical Physics, ETH Hönggerberg, CH-8093 Zurich, Switzerland*
[4]*Bogolyubov Institute for Theoretical Physics, Kiev 03780, Ukraine*

We propose direct experimental tests of the effective models of fractional quantum Hall edge states. We first recall a classification of effective models based on the requirement of anomaly cancellation and illustrate the general classification with the example of a quantum Hall fluid at filling factor $\nu=2/3$. We show that, in this example, it is *impossible* to describe the edge states with only one chiral channel and that there are several inequivalent models of the edge states with two fields. We focus our attention on the four simplest models of the edge states of a fluid with $\nu=2/3$ and evaluate charges and scaling dimensions of quasiparticles. We study transport through an electronic Mach-Zehnder interferometer and show that scaling properties of the Fourier components of Aharonov-Bohm oscillations in the current provide information about the electric charges and scaling dimensions of quasiparticles. Thus, Mach-Zehnder interferometers can be used to discriminate between different effective models of fluids corresponding to the same filling factor. They, therefore, can be used to test fundamental postulates underlying the low-energy effective theory of edge states. An important ingredient of our analysis is the tunneling Hamiltonian of quasiparticles, the form of which is discussed in detail.

I. INTRODUCTION

The quantum Hall effect[1,2] (QHE) is a fascinating example of macroscopic quantum phenomena. It continues to attract much attention among experimental and theoretical physicists. Its large-scale physics is governed by the requirement of anomaly cancellation at the boundary of the system. It provides an example of the so called "holographic principle,"[3,4] which means that the physics of the system confined to some region is encoded in the physics of the degrees of freedom at the boundary of this region (see Fig. 1). Understanding the physics of the quantum Hall (QH) edge states is therefore important for an understanding of the QHE in general.

In the theoretical description of incompressible quantum Hall fluids, the holographic principle manifests itself in the presence of *chiral* edge channels in the low-energy effective theory.[1] These boundary channels are thought to be described by chiral conformal field theory.[6,7] The possible structure of this description is highly constrained by the requirements of locality, the gauge invariance (charge conservation), and the presence of excitations describing electrons (i.e., with quantum numbers of an electron or hole) in the spectrum. These requirements allow one to classify possible effective low-energy models for all observed filling factors.[8,9] However, without taking into account microscopic properties of a particular incompressible QH state, the requirements mentioned above usually do not determine the low-energy effective theory uniquely. Already in examples of incompressible Hall fluids corresponding to simple fractions, such as $\nu=2/3,2/5$, etc., there are several physically inequivalent models satisfying all the requirements even if one limits one's attention to models with the smallest possible number of edge channels. This situation calls for experimental tests of the theory.

There are several proposals to test the QH edge physics. Concrete attempts for such tests have been made in three directions: measurements of the electric charge, of the statistical phase, and of the *scaling dimension* of excitations (quasiparticles and electrons). The scaling dimension of the electron field operator may be tested via the I-V curve at a tunnel junction.[10] This idea has been experimentally implemented in Refs. 11 and 12. The results of these experiments caused an extensive discussion of the well known "2.7 problem."[13] The interpretation of the experiments described in Refs. 11 and 12 is not straightforward, and one may need to take into account the existence of compressible strips[14] at the edge, of disorder,[15] and of electron-phonon interactions.[16] The charge of quasiparticles may be probed by measuring the Fano factor of the tunneling current.[17] Currently, fractional charges have been observed in several experiments[18,19] at different filling factors. Several proposals have been made to use the Fabry-Pérot[20] (FP) and the Mach-Zehnder[21] (MZ) electronic interferometers, which utilize QH edge channels, in place of
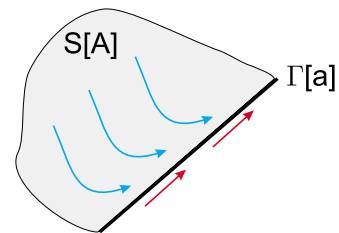

FIG. 1. (Color online) Illustration of the holography in a QH system. The Hall current in the bulk (blue arrows) has an anomaly at the edge (i.e., it is not conserved). This anomaly must be canceled by the anomaly of the edge current (red arrows) (Ref. 5). Therefore, there is an anomalous boundary action $\Gamma[\mathbf{a}]$ that is constrained by the requirement of anomaly cancellation in the bulk effective action $S[\mathbf{A}]$.

optical beams, for measurements of fractional charge and of anyon statistics of quasiparticles.[22–26]

In this work we propose an experiment that would allow one to find out which effective model describes a particular filling factor. The idea is to use an MZ interferometer in order to measure simultaneously the charge and the scaling dimension for each species of quasiparticles that may tunnel through a quantum point contact (QPC). Aharonov-Bohm (AB) oscillations in an MZ interferometer have recently been investigated experimentally in Refs. [27–30] and showed surprising behavior. This has been addressed in several theoretical works.[31–35] The main result of the present work, Eqs. (68) and (70) describing the AB-oscillating contribution to the current through an MZ interferometer at low and high temperatures, shows that the Fourier spectrum of the current as a function of the flux can be used to extract the scaling dimensions and charges of quasiparticles. As an example, we consider the well observed filling factor $\nu = 2/3$ in some detail. We present possible effective models for this filling factor and discuss how they can be distinguished from each other with the help of their spectra of scaling dimensions.

An important property of the $\nu = 2/3$ state is that all minimal models of its edge degrees of freedom contain two edge channels. A similar situation is encountered at $\nu = 2$, where it has been shown that the *long-range* Coulomb interaction between the channels leads to some universalities.[35] In this paper we show that Coulomb interactions fix a freedom in the choice of the edge Hamiltonian, so that scaling dimensions are fully determined by the matrix [Eq. (30)] of statistical phases of electrons (see Sec. V).

We start our paper by recalling the effective theory of QH edges and the classification of possible models. In Sec. II we formulate general requirements that any model must satisfy. We illustrate the implementation of these requirements with the example of fluids with $\nu = 1/(2k+1)$, where a simple hydrodynamic approach can be used, and discuss limitations of this approach. In Sec. III, we discuss general multichannel edge models and recall the construction of local excitations and of their correlation functions. In Sec. IV we explicitly determine the spectrum of scaling dimensions for the most plausible (minimal) models corresponding to $\nu = 2/3$. Section V is devoted to an analysis of the role of Coulomb interactions. Finally, in Sec. VI, we investigate transport trough an electronic MZ interferometer and show how scaling dimensions of excitations can be extracted from AB oscillations of the current through the interferometer. Our form of the tunneling Hamiltonian, which is an important ingredient of the theory, is thoroughly discussed in Appendix C.

II. EFFECTIVE THEORY OF QH EDGES

The effective theory presented in this section provides a description of the low-energy physics of a QH edge. While the correct model of edge states may depend on microscopic details of a two-dimensional electron gas, there are general physical requirements that greatly reduce the number of relevant models.[6,7] These requirements are as follow:

(i) *Cancellation of anomaly.* It is well known that the Chern-Simons theory of an incompressible quantum Hall state is anomalous, i.e., in the presence of a boundary, its gauge variation is given by a nonvanishing boundary term. The effective model of edge states has to be chosen in such a way as to cancel the anomaly of the bulk action in order for the complete theory to be gauge invariant.

(ii) *Existence of an electron operator.* A two-dimensional electron gas consists of electrons. Thus, on a microscopic level, the quantum Hall state is described by an electron wave function. This implies that, in the effective edge theory, there should exist at least one local operator describing the creation or annihilation of an electron or hole, i.e., with a charge e and Fermi statistics.

(iii) *Single-valuedness in the electron positions.* Similarly, because the QH state describes electrons, its wave function must be single-valued in the electron positions, irrespective of whether quasiparticles are present. As a consequence, in the effective theory the mutual statistical phase of a quasiparticle and an electron must be an integer multiple of π.[36]

Below we use these requirements to construct the most simple effective models of QH edge states and to classify various multifield models in Sec. III.

A. Chern-Simons theory and gauge anomaly

First of all, in an incompressible quantum Hall fluid the electric current density, **j**, in the bulk of the system[8] is related to the electromagnetic potential **A** by Hall's law,

$$j^\mu = \sigma_H \epsilon^{\mu\nu\lambda} \partial_\nu A_\lambda, \tag{1}$$

where the constant $\sigma_H = \nu/2\pi$ is the Hall conductivity and the rational number ν is the filling factor (here and below, we use units where $e = \hbar = 1$, and the Einstein summation convention is followed unless specified otherwise). The effective action that leads to Hall's law [Eq. (1)] via $j^\mu = \delta S_{CS}/\delta A_\mu$ is the three-dimensional Chern-Simons action,

$$S_{CS} = \frac{\sigma_H}{2} \int_D d^3r \, \epsilon^{\mu\nu\lambda} A_\mu \partial_\nu A_\lambda, \tag{2}$$

where D is the product of the time axis and some spatial domain.

Action (2) is *anomalous*, i.e., it has a nonvanishing gauge variation in the presence of a boundary. Indeed, gauge transforming the potential $A_\lambda \rightarrow A_\lambda + \partial_\lambda f$ in Eq. (2) by an arbitrary gauge function $f(r)$ and integrating by parts, we obtain the variation of the action,

$$\delta S_{CS} = \frac{\sigma_H}{2} \int_{\partial D} d^2r \, \epsilon^{\nu\lambda} \partial_\nu A_\lambda f. \tag{3}$$

This anomaly originates from the fact that the current [Eq. (1)] is not conserved at the boundary: $\partial_\mu j^\mu \neq 0$ for $r \in \partial D$. Indeed, taking the derivative of Eq. (1), we find that

$$\partial_\mu j^\mu = \sigma_H \epsilon^{\mu\nu\lambda} \partial_\nu A_\lambda \partial_\mu \theta_D, \tag{4}$$

where the function θ_D takes values $\theta_D = 1$ and $\theta_D = 0$ inside and outside the domain D, respectively.

The anomaly must be compensated by boundary degrees of freedom coupled to the electromagnetic field. Namely, the total effective action, after the boundary fields are integrated out, is given by a sum of two terms,
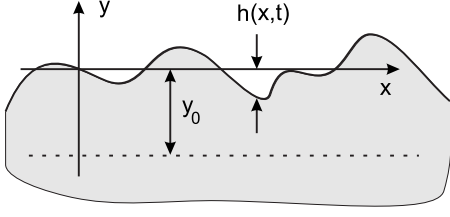
FIG. 2. Deformations of the boundary (thick line) of an incompressible QH fluid (shown in gray) are parameterized by the function $y=h(x,t)$. The auxiliary boundary, where bulk and edge currents match, is indicated by the dashed line $y=-y_0$.

$$S_{\text{tot}}[\mathbf{A}] = S_{CS}[\mathbf{A}] + \Gamma[\mathbf{a}], \tag{5}$$

where $\mathbf{a}$ is the electromagnetic field at the boundary, $\mathbf{a} = \mathbf{A}|_{\partial D}$, and $\Gamma[\mathbf{a}]$ is an anomalous action at the edge.[37] The anomaly in Γ must be such that, under a gauge transformation $a_\lambda \rightarrow a_\lambda + \partial_\lambda f$, this action acquires a variation that cancels exactly the one of the bulk action [see Eq. (3)]: $\delta\Gamma = -\delta S_{CS}$. Under this condition, $S_{\text{tot}}[\mathbf{A}]$ is gauge invariant. Consequently, the edge current $\mathbf{J}$, defined as $J^\mu = \delta(S_{CS}+\Gamma)/\delta a_\mu$, is anomalous, with divergence given by

$$\partial_\mu J^\mu = \sigma_H \epsilon^{\mu\nu}\partial_\mu a_\nu. \tag{6}$$

This divergence cancels the divergence [Eq. (4)] of the bulk current. Below we discuss various models that incorporate these general ideas, starting from a simple hydrodynamical model.

B. Hydrodynamics of incompressible edge deformations

Next, we recall some arguments in Ref. 38, with some modifications taking into account the physics related to long-range Coulomb interactions. Edge excitations can be viewed as deformations of the boundary of an incompressible QH liquid caused by the bulk current flowing toward the edge (see Fig. 2). We parametrize these deformations by a function $y=h(x,t)$ and consider a low-energy limit, so that $h \ll \ell_h$, where ℓ_h is the characteristic wavelength of the deformations. Introducing an auxiliary boundary at a distance y_0 from the edge, with $\ell_h \gg y_0 \gg h$, we represent the edge current $J \equiv J_x$ as the integral $J = \int_{-y_0}^h dy j_x$, and, for the accumulated charge density at the edge, $\rho \equiv J_t$, we write $\rho = n_0 h$, where $n_0 = \nu B/2\pi c$ is the density of the QH liquid and B is the magnetic field value.

An unpleasant aspect of this approach is that the edge current explicitly depends on the auxiliary cutoff at $y=-y_0$. However, we show that the resulting equation of motion for the edge deformations, $h(x,t)$, does not contain this cutoff, and hence the edge current can be redefined to depend on h only. Indeed, charge conservation implies that $\partial_t\rho + \partial_x J = j_y$, where the bulk current density j_y is taken at the boundary $y=-y_0$. Using Eq. (1) and fixing the gauge $a_x=0$, we write $J = \sigma_H[\varphi(x,h) - \varphi(x,-y_0)]$, where $\varphi(x,y)$ is the total electrostatic potential in the plane of the QH fluid. Substituting this expression for the current in the continuity equation, we observe that the terms containing y_0 cancel and the equation of motion takes the form $\partial_t\rho + \sigma_H\partial_x\varphi = 0$. Finally, we split the

potential φ into two parts and write $\partial_x\varphi = \partial_x\varphi_h - \widetilde{E}_x$, where φ_h is the potential at the edge caused by its deformation and $\widetilde{E}_x$ is the external electric field evaluated at $y=h$. While $\widetilde{E}_x$ depends on h, in general, in the low-energy limit it can be taken at $y=0$ to leading order in h. The equation of motion then reads

$$\partial_t\rho + \sigma_H\partial_x\varphi_h = \sigma_H\widetilde{E}_x. \tag{7}$$

After a redefinition of the edge current, $J = \sigma_H\varphi_h$, the cutoff parameter y_0 is gone.

In order to close the equation of motion, we need a relation between the deformation h and the potential φ_h. In the long wavelength limit, we can simply write $\varphi_h = -\partial_\rho H = -(1/n_0)\partial_h H$, where H is the density of electrostatic energy at the edge. This leads to an equation that is, in general, nonlinear in the field ρ. Passing to a low-energy limit, this equation can be linearized, and we arrive at the result

$$\partial_t\rho - v\partial_x\rho = \sigma_H\widetilde{E}_x, \tag{8}$$

where $v = (\sigma_H/n_0^2)\partial_h^2 H(0)$ is the group velocity of the edge excitations. For a stable QH liquid, $\partial_h^2 H(0)$ is positive, and this equation describes the propagation of chiral excitations.

There are two contributions to the electrostatic energy: one is due to the confining potential at the edge and the second one is due to Coulomb interactions. Consequently, the group velocity of edge excitations can be written as a sum of two terms,

$$v = cE/B + \sigma_H V, \tag{9}$$

where the first term is the velocity of drift in the electric field E at the edge of the QH liquid and the second term is proportional to the integral $V = \int dx' U_C(x-x')$ of the Coulomb interaction potential U_C at the edge. This integral is logarithmically divergent and has to be cut off at the distance, d, to the metallic gate and at the microscopic width of the edge a, so that $V \sim \ln(d/a)$.

Here an important remark is in order. The first term in Eq. (9) may be interpreted as a bare velocity, v_0, of excitations. Restoring physical units, it can be estimated as $v_0 \sim (eE/\hbar)l_B^2$, where l_B is the magnetic length. The ratio $\alpha := \sigma_H/v_0 \sim e^2/\hbar v_0$ plays the role of a dimensionless interaction constant. Depending on the confinement at the edge, it is always larger than 1, and in a typical experiment,[21,27–30] $\alpha \gtrsim 10$, which may justify the hydrodynamical model considered here. Moreover, the long-range character of the Coulomb interaction and the fact that $d \gg a$ lead to a large parameter V. As a result, the hydrodynamical charged mode is always present in the spectrum and determines the scaling dimension in nonchiral models, as we demonstrate in Sec. V.

C. Quantization of edge excitations

In order to quantize edge excitations, we consider the total electrostatic energy density $H(\rho) = (v/2\sigma_H)\rho^2$ as a Hamiltonian that generates the homogeneous version of the equation of motion [Eq. (8)] (see Ref. 38). This equation is diagonal in Fourier space, $\partial_t\rho_k - ivk\rho_k = 0$. We therefore write the Hamiltonian as

$$H_k = \frac{v}{\sigma_H} \rho_k \rho_{-k}, \quad (10)$$

where $k > 0$. We identify the "momentum" with $P_k = \rho_k$ and the "coordinate" with $X_k = i\rho_{-k}/\sigma_H k$, so that the equations of motion take the form $\partial_t X_k = \partial H_k / \partial P_k$ and $\partial_t P_k = -\partial H_k / \partial X_k$. Then the canonical commutator $[X_k, P_{k'}] = i\delta_{kk'}$ leads to the commutator $[\rho(x), \rho(x')] = i\sigma_H \partial_x \delta(x - x')$ in real space.

Next, we construct an electron operator. For this purpose it is convenient to represent the charge density in terms of a field $\phi(x)$,

$$\rho(x) = \frac{\sqrt{\nu}}{2\pi} \partial_x \phi(x), \quad (11)$$

with commutation relations

$$[\phi(x'), \phi(x)] = i\pi \, \mathrm{sgn}(x - x'). \quad (12)$$

Here and in the following, we use the term "filling fraction," ν, and "Hall conductivity," σ_H, synonymously; but we always mean the latter. Then the electron operator takes the form

$$\psi = e^{iq\phi} \quad (13)$$

of a local vertex operator (see, e.g., Ref. 39). For this operator to describe the creation and annihilation of an electron or hole, we require that

$$[Q_{\mathrm{em}}, e^{iq\phi}] = e^{iq\phi}, \quad (14)$$

where $Q_{\mathrm{em}} = \int dx \rho = (\sqrt{\nu}/2\pi) \int dx \partial_x \phi$ is the total electric charge at the edge. This requirement implies that the charge of an electron is equal to -1. Using the commutation relations [Eq. (12)] we find that

$$q = 1/\sqrt{\nu}. \quad (15)$$

In addition, electron operator (13) must obey fermionic commutation relations. Applying the Baker-Campbell-Hausdorff formula, we find that $e^{iq\phi(x)} e^{iq\phi(x')} = e^{i\pi q^2} e^{iq\phi(x')} e^{iq\phi(x)}$. Using Eq. (15) and imposing Fermi statistics, we conclude that

$$e^{i\pi/\nu} = -1. \quad (16)$$

This implies that the filling factor is given by $\nu = 1/m$, where m is an odd integer number. In Sec. III, we show that this limitation can be overcome by constructing a multichannel edge model.

According to the third principle formulated at the beginning of this section, the theory may describe quasiparticles with the vertex operators $e^{ip\phi}$ that must be local relative to the electron operator $e^{iq\phi}$. Thus, the statistical phase, θ, of such quasiparticles with respect to an electron has to be an integer multiple of π. Using again commutation relation (12), we arrive at the result that

$$\theta = \pi p \cdot q = \pi n, \quad$$

and the quasiparticle operator takes the form

$$\psi_n = e^{in\sqrt{\nu}\phi(x)}, \quad (17)$$

where n is an integer. Such operators describe Laughlin quasiparticles.[40] The correlation functions of quasiparticle

operators may be calculated easily, with the result $\langle 0|\psi_n^\dagger(x,t)\psi_n(0,0)|0\rangle = (x+vt)^{-\nu n^2}$, where $|0\rangle$ denotes the ground state of a quantum Hall fluid with filling fraction ν. Taking into account that $\nu = 1/m$, the properties of the operators (17) are as follows: they carry a charge $q(n) = n/m$ and have the scaling dimensions $\Delta(n) = n^2/m$. Thus, for an elementary quasiparticle with charge $1/m$, we have that $\Delta_{\mathrm{min}} = 1/m$ and, for an electron, $\Delta_{\mathrm{el}} = m$.

D. Gauge-invariant formulation

In this section we reformulate the theory of edge excitations presented above in a gauge-invariant form suitable for a generalization to multichannel fluids considered in Sec. III. We first rewrite the action $S = \int dt \Sigma_{k>0} [P_k \partial_t X_k - H_k]$ in the linear approximation as

$$S[\phi] = \frac{1}{4\pi} \int dt dx [\partial_t \phi \partial_x \phi - v(\partial_x \phi)^2 + 2\sqrt{\nu}\phi \widetilde{E}_x], \quad (18)$$

where we have included a term describing the coupling to an electric field $\widetilde{E}_x$. This action can easily be generalized to nonlinear edge modes by replacing the term $(v/4\pi)(\partial_x \phi)^2$ with the full Hamiltonian $H(\rho)$.

Next, we replace derivatives $\partial_\mu \phi$ in action (18) with their gauge-invariant form

$$D_\mu \phi \equiv \partial_\mu \phi + \sqrt{\nu} a_\mu \quad (19)$$

and integrate the last term by parts using the relation $\widetilde{E}_x = \epsilon^{\mu\lambda} \partial_\mu a_\lambda$. We then arrive at the following action:

$$S[\phi] = \frac{1}{4\pi} \int dt dx [D_t \phi D_x \phi - v(D_x \phi)^2]$$
$$+ \frac{\sqrt{\nu}}{4\pi} \int dt dx \epsilon^{\mu\lambda} a_\mu \partial_\lambda \phi. \quad (20)$$

It is easy to check that by fixing the gauge $a_x = 0$, one returns to action (18).

The first term in action (20) is invariant under the gauge transformation $a_\mu \to a_\mu + \partial_\mu f$, $\phi \to \phi - \sqrt{\nu}f$. The second term yields the gauge variation $\delta S[\phi] = -(\nu/4\pi) \int dt dx \epsilon^{\mu\lambda} \partial_\mu a_\lambda f$, i.e., the edge action has the desired anomaly: it exactly cancels the anomaly [Eq. (3)] of the bulk action. Thus, the effective theory described by the total action $S_{\mathrm{tot}} = S_{\mathrm{CS}}[\mathbf{A}] + S[\phi]$ is gauge invariant. The boundary effective action $\Gamma[\mathbf{a}]$ in Eq. (5) is obtained by integrating out the field ϕ.

One may then check that the gauge-invariant edge current has the correct anomalous divergence [Eq. (6)]. To see this, we take a variational derivative of the total action with respect to the boundary potential $\mathbf{a}$. This yields the following expression for the edge current:

$$J_t = \frac{\sqrt{\nu}}{2\pi} D_x \phi, \quad J_x = -\frac{\sqrt{\nu}}{2\pi} v D_x \phi. \quad (21)$$

In a gauge where $a_x = 0$, this expression reproduces definition (11) of the charge density as well as the definition of electron operator (13). Indeed, expression (21) for the edge current follows from point splitting of the operator $\psi^\dagger \psi$ in the pres-

ence of an electromagnetic field. Note that the current satisfies the relation $J_x = -vJ_t$, which exhibits its chiral nature. Finally, by varying action (20) with respect to ϕ, we obtain the equation of motion for ϕ, which is used to evaluate the divergence of the current [Eq. (21)]. We then arrive at Eq. (6), i.e., the edge current has the desired anomalous divergence.

We conclude that the hydrodynamical model, when applied to QH states with $\nu = 1/m$, where m is an odd integer, satisfies all the requirements formulated at the beginning of this section. In Sec. III, we show that by considering more than one bosonic mode at the edge of a QH liquid, one can construct effective edge models for general filling factors.

III. MULTICHANNEL EDGE MODELS

As shown in Sec. II C, a single-channel hydrodynamical model of the QH edge cannot describe all observed filling fractions. We therefore consider more general multichannel edge models. A natural generalization of single-field action (20) to many fields is given by

$$S[\phi_i] = \frac{1}{4\pi} \sum_i \int dtdx [\sigma_i D_t \phi_i D_x \phi_i - v_i (D_x \phi_i)^2]$$
$$+ \frac{1}{4\pi} \sum_i \int dtdx [Q_i \epsilon^{\mu\lambda} a_\mu \partial_\lambda \phi_i], \quad (22)$$

where $\sigma_i = \pm 1$ encodes the chirality of the ith channel, v_i is the propagation speed, and Q_i is the constant of electromagnetic coupling of the field ϕ_i. The covariant derivatives are defined by $D_\mu \phi_i = \partial_\mu \phi_i + \sigma_i Q_i a_\mu$. We emphasize that any quadratic gauge-invariant action for chiral bosons can be brought to the unique form [Eq. (22)] by redefining the fields. Here we consider the general case with different propagation speeds, v_i, for different edge modes because recent experiments[27–30] show that this can occur.

The requirement of anomaly cancellation for edge action (22) implies that

$$\sum_i \sigma_i Q_i^2 = \nu. \quad (23)$$

One can see that, in contrast to a single-channel edge where the last term in action (20) is uniquely fixed by the Hall conductivity, in the multichannel situation only the "length" of the vector Q_i is fixed to be $\sqrt{\nu}$, while, at this point, its direction is still arbitrary.

A. Kinematics of edge models

In order to check the second physical requirement, the existence of excitations with the quantum numbers of electron, we consider a general vertex operator

$$\psi = \exp\left(i \sum_j q_j \phi_j\right), \quad (24)$$

where q_j are some constants. Taking into account commutation relations

$$[\partial_x \phi_i(x,t), \phi_j(x',t)] = -2\pi i \sigma_i \delta_{ij} \delta(x - x'), \quad (25)$$

which follow from Eq. (22), we find that the statistical phase of operator (24) is given by

$$\theta = \pi \sum_i \sigma_i q_i q_i. \quad (26)$$

The electric charge operator is given by $Q_{\text{em}} = (1/2\pi) \sum_i Q_i \int dx \partial_x \phi_i$, in accordance with Eq. (22). Therefore, one finds with the help of Eq. (25) that the charge of field operator (24) is given by

$$Q_{\text{em}} = \sum_i \sigma_i Q_i q_i. \quad (27)$$

Here, as in the integer QHE, it is possible to have several electron operators differing from each other by some quantum numbers. The origin of these quantum numbers is discussed in Appendix D. We label different electron operators by an additional index α,

$$\psi_\alpha = \exp\left(i \sum_j q_{\alpha j} \phi_j\right), \quad (28)$$

and assume that the number of electrons coincides with the number of channels.[41] All electron fields must have a unit charge, which implies that

$$\sum_i \sigma_i Q_i q_{\alpha i} = 1, \quad (29)$$

and appropriate relative statistical phases, $\pi K_{\alpha\beta}$, compatible with relative locality and Fermi statistics. This implies that the numbers

$$K_{\alpha\beta} = \sum_i \sigma_i q_{\alpha i} q_{\beta i} \quad (30)$$

must be integers and that, for $\alpha = \beta$, these numbers must be odd integers.

In Fig. 3 we schematically illustrate conditions (29) and (30) for the simple example of two channels with the same chiralities. One sees that in contrast to the single-channel case, in multichannel models there is a freedom in choosing electron operators even if the coupling constants Q_i are fixed. This freedom implies that different microscopic QH wave functions may lead to the same action in the low-energy limit. In this case the low-energy projections of electronic operators may, in principle, be different. In fact, multichannel models are fully determined by the numbers q_α^i, while the values of coupling constants Q_i can be obtained by solving Eq. (29),

$$Q_i = \sigma_i \sum_\alpha q_{i\alpha}^{-1}. \quad (31)$$

The physical requirements for the effective theory can therefore be formulated as constraints on the q matrix. Namely, the requirement that elements of the matrix K given by Eq. (30) are integer numbers has to be accompanied by the condition that
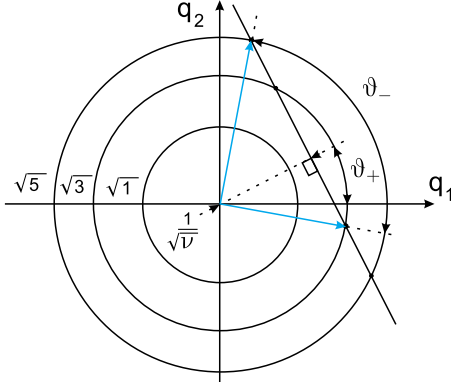
FIG. 3. (Color online) Schematic illustration of the conditions for electron operators in a chiral two-field model. The requirement for the statistical phase of an electron operator to be fermionic is $q_{\alpha 1}^2 + q_{\alpha 2}^2 = 2k+1$. This means that the end points of vectors $\mathbf{q}_\alpha \equiv \{q_{\alpha i}\}$ (drawn in blue) lie on the circle of radius $\sqrt{2k+1}$. The condition of unit charge, $Q_1 q_{\alpha 1} + Q_2 q_{\alpha 2} = 1$, implies that the end points of vectors $\mathbf{q}_\alpha$ lie on the line perpendicular to the vector $\mathbf{Q} \equiv \{Q_i\}$. The length of this vector is fixed by the anomaly cancellation condition (23), namely, $|\mathbf{Q}| = \sqrt{\nu}$. Therefore, the distance from the line through the end points of the vectors $\mathbf{q}_\alpha$ to the origin is fixed to be $1/\sqrt{\nu}$. We denote the angle between $\mathbf{Q}$ and the q_1 axis by ϑ_+, and the angle between the electron vectors by ϑ_-.

$$\sum_{\alpha,\beta} K_{\alpha\beta}^{-1} = \nu, \tag{32}$$

which follows from the requirement of anomaly cancellation [Eq. (23)] and from Eq. (31).

Note that we have reformulated the constraints on the matrix q as constraints on the matrix K. In Sec. III B, we show that the *kinematic* information about an effective model is encoded in the matrix K. More precisely, the spectra of statistical phases and charges of quasiparticles are entirely determined by K. For every filling factor this matrix takes values from a discrete set. For instance, in two-channel models this corresponds to the discrete set of choices of lengths of electronic vectors $\mathbf{q}_\alpha$ and their relative angle ϑ_- (see Fig. 3). From relation (30) it follows that the remaining freedom in the matrix q for a given matrix K is the angle ϑ_+ of the simultaneous rotation of two vectors $\mathbf{q}_\alpha$. In Sec. III B we show that the *dynamical* properties of the model, such as the correlation functions, are not determined by the matrix K only but depend on the whole matrix q, e.g., on the angle ϑ_+ in the case of two fields.

B. Local excitations

Next, we determine all quasiparticle operators in accordance with the requirement that they have integer statistical phases relative to all electron fields [Eq. (28)]. Quasiparticle operators are vertex operators of the form

$$\psi = \exp\left(i \sum_j p_j \phi_j \right). \tag{33}$$

Their statistical phases relative to electronic fields are given by

$$\theta_{pq_\alpha} = \pi \sum_i \sigma_i p_i q_{\alpha i} = \pi n_\alpha. \tag{34}$$

The numbers n_α must be integers. The solution of Eq. (34),

$$p_i = \sigma_i \sum_\beta q_{i\beta}^{-1} n_\beta, \tag{35}$$

is a linear combination with integer coefficients. Therefore, the whole set of allowed quasiparticle operators forms a lattice, which is dual to the lattice spanned by electronic vectors $q_{\alpha i}$ (see Appendix E and Ref. 8 for a detailed discussion of this point).

It is interesting to note that the statistical phase and the charge of a quasiparticle operator labeled by the numbers n_α can be expressed solely in terms of the matrix K. For the statistical phase we have that

$$\frac{\theta}{\pi} = \sum_i \sigma_i p_i p_i = \sum_{\alpha,\beta} n_\alpha K_{\alpha\beta}^{-1} n_\beta. \tag{36}$$

It also follows from Eqs. (31) and (35) that the charge of the operator in Eq. (33) is given by

$$Q_{em} = \sum_i \sigma_i Q_i p_i = \sum_{\alpha\beta} K_{\alpha\beta}^{-1} n_\beta. \tag{37}$$

Note that the summation over the index α in this equation may be viewed as the multiplication by the vector $(1, 1, \ldots, 1)$.

It may happen that different matrices K generate the same set of quasiparticles. This is the case when corresponding electronic vectors $q_{\alpha i}$ form different bases of the same lattice (see the discussion in Appendix E). An example of such an equivalence is depicted in Fig. 4. In the language of matrices q, an equivalence is the consequence of the fact that an integral transformation $q'_{\alpha i} = \Sigma_\beta T_{\alpha\beta} q_{\beta i}$ (i.e., one with the elements $T_{\alpha\beta}$ and $T_{\alpha\beta}^{-1}$ being integer numbers) is nothing but an automorphism of the integral lattice generated by a change of basis. Using definition (30), this equivalence may also be written as

$$K \leftrightarrow K' = TKT^T. \tag{38}$$

Since the matrix T transforms an electronic basis, it preserves the charge of an electron. Taking into account Eq. (37), this important condition implies that the matrix T should preserve the vector $(1, 1, \ldots, 1)$.

In conclusion, we propose the following strategy to find inequivalent models for a given filling factor. First of all, one must find all solutions, K, of Eq. (32) for a given ν up to equivalence defined by proper integral transformations [Eq. (38)]. This procedure fixes the kinematic content of the theory.[42] Second, one must fix those parameters that are not constrained by the general conditions formulated at the beginning of Sec. II. These parameters are the propagation speeds, v_i, of chiral edge modes. Finally, one should choose an explicit basis, $\mathbf{q}_\alpha$, of vectors labeling electron field operators and consistent with the chosen matrix K.

C. Scaling dimensions of local excitations

We conclude this section by presenting the correlation functions of the quasiparticle operators [Eq. (33)]. A detailed
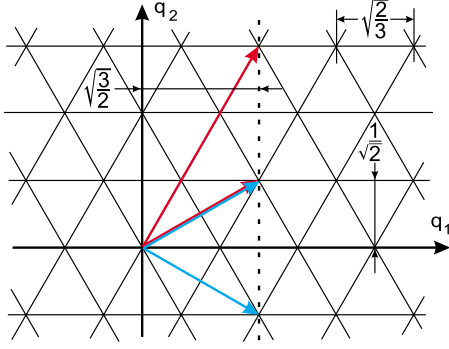
FIG. 4. (Color online) Illustration of equivalence of two QH lattices. For two channels of different chiralities, the statistical phase satisfies $\theta/\pi = q_1^2 - q_2^2$. Using this fact, one can easily see that the red vectors correspond to K matrix (49) and the blue vectors correspond to the K matrix (50). Note that these pairs of vectors are just different bases of the same lattice (which is dual to the one shown in the figure). Therefore, the spectra of statistical phases in models (49) and (50) are identical. Finally, the dashed line constrains the charge of the electrons to be 1. The fact that all electron vectors lie on the same line implies that the constants Q_i are the same for both models. This means that the charges $Q_{em} = \Sigma q_i Q_i$ of excitations in one model coincide with those in the second model. Here, we choose the angle $\vartheta_+ = 0$, in accordance with the conclusion of Sec. V.

calculation of this function is contained in Appendix B and yields

$$\langle 0 | \psi^\dagger(x,t) \psi(0,0) | 0 \rangle \propto e^{i\varphi_0(\mathbf{n})} \prod_i (x + \sigma_i v_i t)^{-\delta_i(\mathbf{n})}, \quad (39)$$

where the exponents are given by

$$\delta_i(\mathbf{n}) = p_i^2 = \left[\sum_\alpha q_{\alpha i}^{-1} n_\alpha \right]^2. \quad (40)$$

Here $\mathbf{n} \equiv \{n_\alpha\}$ and φ_0 is a phase, the exact value of which is discussed in Sec. VI.

The scaling dimension of the correlation function, defined via its long-time behavior, is given by

$$\Delta(\mathbf{n}) = \sum_i \delta_i(\mathbf{n}). \quad (41)$$

Expressed in terms of the q matrix, it reads

$$\Delta(\mathbf{n}) = \sum_i p_i^2 = \sum_{\alpha,\beta} n_\alpha (qq^T)^{-1}_{\alpha\beta} n_\beta. \quad (42)$$

An explicit calculation of Δ in the nonchiral case with two fields is given in Appendix A. The scaling dimensions Δ are not fully determined by the matrix K, while according to Eq. (36), the statistical phases

$$\frac{\theta}{\pi} = \sum_i \delta_i \sigma_i \quad (43)$$

are given by the matrix K. Comparing Eqs. (41) and (43) we conclude that $\Delta \geq \theta/\pi$, where equality holds in a purely chiral case.

IV. MINIMAL MODELS FOR $\nu = 2/m$ AND SCALING DIMENSIONS OF THEIR QUASIPARTICLE FIELDS

In this section we apply the ideas discussed above to the particular case of filling factors $\nu = 2/m$. In Ref. 15 it has been shown that models with a large number of edge channels may be unstable under the influence of disorder. To avoid such complications, we limit our analysis to models with the smallest possible number of fields (see also the discussion at the end of Appendix D). Moreover, we consider models with minimal statistical phases of electron field operators because they are most relevant physically.[43]

A direct solution of Eq. (32) is complicated. Fortunately, in Ref. 8, some general results have been proven for the case where the statistical phases of electron operators are smaller than 7π: all two-field models for $\nu = 2/m$ are described by matrices K of the following form:

$$K_a = \begin{pmatrix} a & b \\ b & a \end{pmatrix}. \quad (44)$$

Equation (32) then imposes the following constraint on matrix (44):

$$\nu = \frac{2a - 2b}{a^2 - b^2} = \frac{2}{a + b}. \quad (45)$$

Thus, for $\nu = 2/m$, the parameters a and b are related by $a + b = m$, where the odd integer a enumerates the models.

For a purely chiral model, the scaling dimensions of correlation functions [Eq. (42)] are given by the statistical phases. Therefore, for a K matrix of form (44), they are given by the expression

$$\Delta(\mathbf{n}) = \frac{1}{a^2 - b^2} [a(n_1^2 + n_2^2) - 2bn_1n_2] \quad (46)$$

and the charge of excitations can be evaluated as

$$Q_{em} = \frac{n_1 + n_2}{m}. \quad (47)$$

For nonchiral models, the expression for the charges of quasiparticles remains the same, while the scaling dimensions [Eq. (42)] depend on an additional parameter, ϑ_+ (see Appendix A). In Sec. IV, we show that, in the limit of strong Coulomb interactions, this parameter takes the universal value $\vartheta_+ = 0$. The scaling dimensions are then given by

$$\Delta(\mathbf{n}) = \frac{1}{b^2 - a^2} [b(n_1^2 + n_2^2) - 2an_1n_2]. \quad (48)$$

We have already mentioned that any two-field solution of Eq. (32) corresponds to one of the matrices (44) up to equivalence described by the transformations (38). An important example is the K matrix proposed, e.g., in Ref. 44,

$$K = \begin{pmatrix} 1 & 0 \\ 0 & -3 \end{pmatrix}. \quad (49)$$

This matrix describes a nonchiral model of the $\nu = 2/3$ state obtained by particle-hole conjugation of the $\nu = 1/3$ state. In this state, the density at the edge first increases to $\nu = 1$ and

TABLE I. Scaling dimensions of excitations in different models of the $\nu=2/3$ state. For each model described by a matrix K_a, we provide the general expression for the scaling dimensions $\Delta(\mathbf{n})$ of quasiparticle operators labeled by pairs of integer numbers (n_1,n_2). The minimal values Δ_q for excitations of charge q, as well as the scaling dimensions of electron operators, are listed in the right column.

K_a	$\Delta(\mathbf{n})$	$\Delta_0, \Delta_{1/3}, \Delta_{2/3}, \Delta_1, \Delta_{el}$
K_5	$\frac{1}{21}[5(n_1^2+n_2^2)+4n_1 n_2]$	$\frac{6}{21}, \frac{5}{21}, \frac{2}{3}, \frac{11}{7}, 5$
K_3	$\frac{1}{3}(n_1^2+n_2^2)$	$\frac{2}{3}, \frac{1}{3}, \frac{2}{3}, \frac{5}{3}, 3$
K_1	$\frac{2}{3}(n_1^2+n_2^2-n_1 n_2)$	$2, \frac{2}{3}, \frac{2}{3}, 2, 2$
K_{-1}	$\frac{2}{15}[2(n_1^2+n_2^2)+n_1 n_2]$	$\frac{6}{15}, \frac{4}{15}, \frac{2}{3}, \frac{8}{5}, 4$

then drops to zero, which implies the presence of two edge channels with opposite chiralities. Another K matrix for $\nu=2/3$ state appears in the context of the composite fermion approach,[45]

$$K=\begin{pmatrix} 1 & 2 \\ 2 & 1 \end{pmatrix}. \tag{50}$$

It turns out that model (49) is equivalent to Eq. (50) in the sense of Eq. (38). Indeed, one can apply an integral change of variables transforming one K matrix into the other one,

$$\begin{pmatrix} 1 & 0 \\ 2 & -1 \end{pmatrix}\begin{pmatrix} 1 & 0 \\ 0 & -3 \end{pmatrix}\begin{pmatrix} 1 & 2 \\ 0 & -1 \end{pmatrix}=\begin{pmatrix} 1 & 2 \\ 2 & 1 \end{pmatrix}.$$

This transformation is of the type of Eq. (38) because it has the property that

$$\begin{pmatrix} 1 & 0 \\ 2 & -1 \end{pmatrix}^{-1}=\begin{pmatrix} 1 & 0 \\ 2 & -1 \end{pmatrix}$$

and it leaves the vector $(1,1)$ invariant. The equivalence of these two models is illustrated in Fig. 4.

For $\nu=2/3$, the matrices (44) with the smallest diagonal elements (i.e., with smallest statistical phases of electron operators) are the following ones:

$$K_3=\begin{pmatrix} 3 & 0 \\ 0 & 3 \end{pmatrix}, \quad K_5=\begin{pmatrix} 5 & -2 \\ -2 & 5 \end{pmatrix} \tag{51}$$

and

$$K_1=\begin{pmatrix} 1 & 2 \\ 2 & 1 \end{pmatrix}, \quad K_{-1}=\begin{pmatrix} -1 & 4 \\ 4 & -1 \end{pmatrix}. \tag{52}$$

Note that the matrices (52) have negative determinants, and hence, in contrast to the matrices (51), they describe nonchiral states. We summarize the values of scaling dimensions of excitations in models (51) and (52) in Table I.

It is important to note that, for every model, the minimal scaling dimension is $\Delta_{\min}=\Delta_{1/3}$, i.e., the operator of the Laughlin quasiparticle is the most relevant one. We note that between four models, the model K_1 is presumably most stable with respect to disorder because it has the largest scaling dimension Δ_0. Moreover, the electron operator in this model is the most relevant operator among operators with
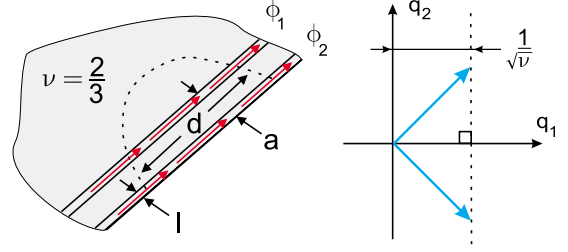

FIG. 5. (Color online) Illustration of the effects of the strong long-range Coulomb interaction. Left panel: important spatial scales at the QH edge are shown: the width of the channels l, the distance between two channels a, and the screening length of the Coulomb interaction d. The universal limit is achieved when $d\gg a,l$. Right panel: possible configuration of electronic excitations (blue vectors) in the universal strong interaction limit. Exactly this situation arises at $\nu=2$, as shown in Ref. 35.

unit charge. In addition, numerical simulations[46] and some microscopic considerations[44] confirm that the model with matrix K_1 is most likely to describe the $\nu=2/3$ state. However, some signs of a phase transition in the $\nu=2/3$ state have been observed.[47] This indicates that other models may also be realized under certain conditions (see Ref. 8).

V. ROLE OF COULOMB INTERACTIONS

We have shown in Sec. III C (see also Appendix A) that, in the nonchiral case, the scaling dimensions of excitations depend not only on the kinematic structure of the theory encoded in the K matrix but also on the angle ϑ_+. This angle parametrizes the relation between the propagating modes and the electron operators. There is, however, an important class of systems in which this parameter appears to be uniquely and universally fixed. This is, for instance, the case in a system with two edge modes and strong Coulomb interactions. This fact has been discussed in Ref. 35. The results of the analysis in Ref. 35 are essentially in perfect agreement with the experimental data in Refs. 27–30. Although in Ref. 35 only the case $\nu=2$ is considered, we will show below that the conclusion of this analysis applies without significant changes to fractional fluids too.

Let us assume that effects of disorder are negligible. This may be a reasonable assumption for an electronic MZ interferometer, the size of which is typically only a few microns. In this case, the generic form of the Hamiltonian is given by a sum of the free Hamiltonian, the Coulomb interaction term, and a term describing the interaction with an external electromagnetic field a_μ,

$$\mathcal{H}=\mathcal{H}_0+\mathcal{H}_C+\mathcal{H}_{int}[\mathbf{a}]. \tag{53}$$

We show below that the actual form of the free Hamiltonian $\mathcal{H}_0$ is not important.

Assuming the distance, a, between the edge channels to be of the order of their thickness, l, or smaller (see Fig. 5 for notations), the Coulomb interaction term can be written as

$$\mathcal{H}_C = (1/2) \int dx dx' \rho_{em}(x) U_C(x-x') \rho_{em}(x'), \qquad (54)$$

where $\rho_{em}(x)$ is the total one-dimensional (1D) charge density at the point x and $U_C(x-x')$ is the Coulomb potential. We further assume that the interaction is screened at distances d, with $L \gg d \gg a$, where L is the size of the interferometer. This screening can occur due to the presence of the back gate or the massive air bridge (see Ref. 35 for a more detailed discussion). As a consequence, we can neglect the dispersion of the Coulomb interaction and write $U_C(x-y) = V\delta(x-y)$, where the interaction constant, $V \sim \ln(d/a)$, is large. Finally, the interaction with an external electromagnetic field is described by

$$\mathcal{H}_{int}[\mathbf{a}] = -\int dx \rho_{em}(x) a_t(x) \qquad (55)$$

in the gauge $a_x = 0$.

In the limit when $\ln(d/a) \gg 1$, the Coulomb interaction exceeds the correlation energy. One of the most important consequences of this fact is that, independently of the form of free Hamiltonian, the full Hamiltonian is diagonal in the basis where one mode, ϕ_1, is charged, with $Q_1/2\pi \partial_x \phi_1 = \rho_{em}$, and the other one, ϕ_2, is a dipole mode of total charge zero. Thus, we can write

$$\mathcal{H} = \frac{1}{4\pi} \sum_i \int v_i (\partial_x \phi_i)^2 - \frac{1}{2\pi} Q_1 \int a_t \partial_x \phi_1, \qquad (56)$$

where the speed of the charged mode, $v_1 = \sigma_H V$, is much larger than the speed v_2 of the dipole mode determined by the free Hamiltonian (see the discussion at the end of Sec. II B). Comparing Eq. (56) with Eq. (22), we conclude that $Q_2 = 0$, which means that the dipole mode does not couple to the external electromagnetic field. The condition of the anomaly cancellation [Eq. (23)] therefore implies that $Q_1 = \sqrt{\nu}$. Thus, the angle between the vector Q and the q_1 axis is fixed to the universal value $\vartheta_+ = 0$. This is illustrated graphically in Fig. 5.

VI. EXPERIMENTAL DETERMINATION OF CHARGES AND SCALING DIMENSIONS OF QUASIPARTICLES

We have shown in Sec. IV that, for the filling factor $\nu = 2/3$, there are several possible models satisfying all the physical requirements formulated in Sec. II. It is worth noticing that all these models have the same minimal fractional charge, 1/3, but different spectra of scaling dimensions. The experiment proposed in this section may allow one to determine scaling dimensions and, as a result, to identify the physically relevant model of the QH edge. This experiment is based on the idea to make use of an electronic MZ interferometer.

Electronic MZ interferometers have been realized and investigated experimentally in Refs. 27–30. The experimental sample consists of a two-dimensional electron gas confined to a region of the shape of a so called *Corbino disk* (see Fig. 6). In the QHE regime, several effectively one-dimensional conducting channels are formed at the edge. The modes in
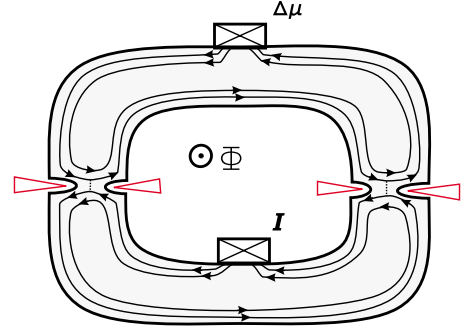

FIG. 6. (Color online) A Mach-Zehnder interferometer is schematically shown as a Corbino disk, containing a two-dimensional electron gas, shown in gray shadow. In a strong magnetic field, at a filling factor $\nu = 2/3$, two 1D chiral channels are formed at the edges and propagate along the boundaries of the two-dimensional electron gas (shown by thin black lines). Both channels are partially transmitted at the left and right QPCs. A bias voltage $\Delta\mu$, applied at the upper Ohmic contact, causes a current I to flow to the lower Ohmic contact. This current is caused by scattering of quasiparticles at the QPCs and involves an interference contribution sensitive to the magnetic flux Φ that can be changed by a slight modulation of the length of one of the arms.

these edge channels are used as beams in the electronic MZ interferometer, while two QPCs serve as beam splitters. Two Ohmic contacts connected to the Corbino disk emit and absorb electrons. One contact is biased with a voltage $\Delta\mu > 0$ and the other one is grounded and serves as a sink for a current I.

There are two paths for quasiparticles to travel from the upper Ohmic contact to the lower one. The first possibilities are to pass the left QPC and to be reflected off the right QPC. The second possibilities are to bounce off the left QPC and then to pass the right one. It is easy to see that a nonzero magnetic flux is enclosed by these two paths. Consequently, the current I oscillates as a function of the magnetic flux through the interferometer. The AB flux may be varied with the help of a modulation gate near one of the arms of the interferometer that can slightly change the length of this arm (see also the discussion in Appendix C 2).

We assume that there are several types of excitations, labeled by integers n_α, which can tunnel between the arms at the QPCs. They are created by operators

$$\psi_{\mathbf{n}} = \exp\left(i \sum_j p_j(\mathbf{n}) \phi_j\right), \quad p_j(\mathbf{n}) = \sigma_j \sum_\alpha q_{\alpha j}^{-1} n_\alpha. \quad (57)$$

Thus, the tunneling Hamiltonian is given by

$$\mathcal{H}_T = \sum_{\ell,\mathbf{n}} t_{\ell,\mathbf{n}} \psi_{U,\mathbf{n}}^\dagger(x_\ell) \psi_{D,\mathbf{n}}(x_\ell) + \text{H.c.} \equiv \sum_{\ell,\mathbf{n}} (A_{\ell,\mathbf{n}} + A_{\ell,\mathbf{n}}^\dagger), \quad (58)$$

where the subscripts U, D indicate that the quasiparticles are created and annihilated at the upper arm and at the lower arm of the interferometer (see Fig. 7), i.e., at the outer edge and at the inner edge of the Corbino disk. Moreover, $t_{\ell,\mathbf{n}}$ are the tunneling amplitudes of particles of type $\mathbf{n}$ at the left and
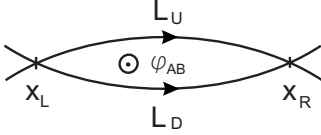
FIG. 7. Schematic representation of the MZ interferometer. Quasiparticles of electric charge $Q_{\text{em}}(\mathbf{n})$ tunnel at points x_L and x_R, with tunneling amplitudes $t_{L,\mathbf{n}}$ and $t_{R,\mathbf{n}}$, respectively. They propagate along paths of length L_U and L_D and acquire an Aharonov-Bohm phase $\varphi_{\text{AB}} = 2\pi Q_{\text{em}}(\mathbf{n})\Phi/\Phi_0$. The upper arm is biased with $\Delta\mu$.

right QPCs, $\ell = L, R$. These amplitudes include the AB phase shift,

$$\arg\frac{t_{R,\mathbf{n}}}{t_{L,\mathbf{n}}} = 2\pi i Q_{\text{em}}(\mathbf{n})\frac{\Phi}{\Phi_0}, \tag{59}$$

where Φ is the flux through the interferometer and $\Phi_0 = hc/e$ is the flux quantum. Our choice of tunneling Hamiltonian requires justification, which is presented and discussed in detail in Appendix C.

The current through the MZ interferometer is defined as a rate of change in the electromagnetic charge $Q_{\text{em}} = \Sigma_i (Q_i/2\pi)\int dx\, \partial_x \phi_i$ in one of the arms of the interferometer (see Fig. 7 for notations),

$$\hat{I} = i[\mathcal{H}, Q_{\text{em}}] = i[\mathcal{H}_T, Q_{\text{em}}]. \tag{60}$$

Calculating the commutator in Eq. (60) with $\mathcal{H}_T$ as in Eq. (58), we arrive at the following expression for the current operator:

$$\hat{I} = \sum_{\ell,\mathbf{n}} i Q_{\text{em}}(\mathbf{n})(A_{\ell,\mathbf{n}} - A_{\ell,\mathbf{n}}^\dagger). \tag{61}$$

We evaluate the average current, $I = \text{Tr}(\hat{\rho}\hat{I})$, to leading order in the tunneling amplitudes t_ℓ,

$$I = \sum_{\ell,\ell',\mathbf{n}} Q_{\text{em}}(\mathbf{n}) \int_{-\infty}^{+\infty} dt \langle [A_{\ell,\mathbf{n}}^\dagger(t), A_{\ell',\mathbf{n}}(0)] \rangle, \tag{62}$$

where the operators $A_{\ell,\mathbf{n}}^\dagger$, $A_{\ell,\mathbf{n}}$ are taken in the interaction representation and averaging is defined as $\langle \cdots \rangle := \text{Tr}\,\hat{\rho}_0(\cdots)$, where $\hat{\rho}_0$ is the density operator of disconnected arms. In Eq. (62) we have taken into account that $\langle \psi_{\mathbf{n}}^\dagger \psi_{\mathbf{m}} \rangle \propto \delta_{\mathbf{n},\mathbf{m}}$, which is a consequence of zero modes.

It is easy to see that expression (62) for the current is a sum of four terms: $I = \Sigma_{\ell\ell'} I_{\ell\ell'}$, where $\ell, \ell' = L, R$. The first two terms,

$$I_{\ell\ell} = \sum_{\mathbf{n}} Q_{\text{em}}(\mathbf{n}) \int_{-\infty}^{+\infty} dt \langle [A_{\ell,\mathbf{n}}^\dagger(t), A_{\ell,\mathbf{n}}(0)] \rangle, \tag{63}$$

correspond to incoherent tunneling at either one of the two QPCs. The other two terms depend on the magnetic flux Φ and lead to interference:

$$I_\Phi \equiv I_{LR} + I_{RL} = 2\sum_{\mathbf{n}} Q_{\text{em}}(\mathbf{n})\text{Re} \int_{-\infty}^{+\infty} dt \langle [A_{R,n}^\dagger(t), A_{L,n}(0)] \rangle. \tag{64}$$

We focus our attention on the interference term because it allows us to discriminate between contributions from different excitations. Using Eq. (58), we write

$$I_\Phi = 2\sum_{\mathbf{n}} Q_{\text{em}}(\mathbf{n})\text{Re}\, t_{L,\mathbf{n}} t_{R,\mathbf{n}}^* \int_{-\infty}^{+\infty} dt \{\langle \psi_{D,\mathbf{n}}(x_R,t)\psi_{D,\mathbf{n}}^\dagger(x_L,0)\rangle$$
$$\times \langle \psi_{U,\mathbf{n}}^\dagger(x_R,t)\psi_{U,\mathbf{n}}(x_L,0)\rangle - \langle \psi_{D,\mathbf{n}}^\dagger(x_L,0)\psi_{D,\mathbf{n}}(x_R,t)\rangle$$
$$\times \langle \psi_{U,\mathbf{n}}(x_L,0)\psi_{U,\mathbf{n}}^\dagger(x_R,t)\rangle\}. \tag{65}$$

The correlation functions are evaluated in Appendix B. The result is

$$i\langle \psi_{\mathbf{n}}^\dagger(x,t)\psi_{\mathbf{n}}(0,0)\rangle \propto \exp[i\varphi_0(\mathbf{n})]$$
$$\times \prod_i \left\{ \frac{v_i}{\pi T}\sinh\left[\pi T\left(t + \sigma_i\frac{x}{v_i}\right)\right]\right\}^{-\delta_i(\mathbf{n})}. \tag{66}$$

The phase $\varphi_0(\mathbf{n})$ in this equation is determined by the structure of zero modes and requires a separate consideration. Introducing zero modes ϕ_i and π_i via $\phi_i(x) = \phi_i + 2\pi x\pi_i$ +osc., we write the corresponding term in Eq. (56) as $\mathcal{H}_0 = \pi W\Sigma_i v_i \pi_i^2$, where W is the total size of the system. The total charge at an edge is given by $Q_{\text{em}} = W\langle\pi_1\rangle$. The expectation values of the zero modes can be related to the applied voltage bias $\Delta\mu$ by appealing to the well known electrostatic formula $\Delta\mu = \delta\langle\mathcal{H}_0\rangle/\delta Q_{\text{em}}$. From this equation it follows that $\langle\pi_1\rangle = \Delta\mu/v_1$, while for the dipole mode $\langle\pi_2\rangle = 0$ because it is not biased.[48] We assume that charge fluctuations are negligible due to the large capacitances of edge channels connected to Ohmic contacts. Thus, the contribution of zero modes is given by $\langle e^{2\pi i p_j \pi_j(x+\sigma_j v_j t)}\rangle = e^{2\pi i p_j \langle\pi_j\rangle(x+\sigma_j v_j t)}$. Substituting the expectation values of zero modes, we find the phase of correlation function (66),

$$\varphi_0(\mathbf{n}) \equiv \sum_i p_i \langle\pi_i\rangle(x + \sigma_i v_i t) = \Delta\mu\left(t + \sigma_i\frac{x}{v_1}\right)\sum_\alpha q_{\alpha 1}^{-1} n_\alpha. \tag{67}$$

Apparently, this phase is linear in the bias $\Delta\mu$.

In the zero-temperature limit, $T = 0$, the correlation functions are given by formula (39). The time integral in Eq. (65), at small biases $\Delta\mu \ll v_i/L_\alpha$, $\alpha = U, D$, then yields

$$I_\Phi = \sum_{\mathbf{n}} C_{\mathbf{n}}(\Delta\mu)^{2\Delta(\mathbf{n})-1}\cos\left[2\pi Q_{\text{em}}(\mathbf{n})\frac{\Phi}{\Phi_0}\right], \tag{68}$$

where the $C_{\mathbf{n}}$ are some (unimportant) constants. In the high-temperature limit, correlation function (66) scales as

$$i\langle \psi_{\mathbf{n}}^\dagger(x,t)\psi_{\mathbf{n}}(0,0)\rangle \propto \exp\left[-\sum_i \pi T\delta_i(\mathbf{n})\left|t + \sigma_i\frac{x}{v_i}\right|\right]. \tag{69}$$

The oscillating part of the current at small bias then takes the following form (see Appendix B):

$$\frac{I_\Phi}{\Delta\mu} = \sum_{\mathbf{n}} C'_{\mathbf{n}} T^{2\Delta(\mathbf{n})-1} e^{-\pi T/T_0(\mathbf{n})} \cos\left[2\pi Q_{\mathrm{em}}(\mathbf{n})\frac{\Phi}{\Phi_0}\right],$$

(70)

where the $C'_{\mathbf{n}}$ are constants and the characteristic energy scale is given by

$$\frac{1}{T_0(\mathbf{n})} = \min_{\alpha',i'} \sum_{\alpha,i} \delta_i(\mathbf{n}) \left|\frac{\sigma_i L_\alpha}{v_i} - \frac{\sigma_{i'} L_{\alpha'}}{v_{i'}}\right|.$$

(71)

For a symmetric interferometer, in the limit $v_1 \gg v_2$, this expression simplifies to

$$T_0^{-1}(\mathbf{n}) = \min[\delta_1(\mathbf{n}), \delta_2(\mathbf{n})]\frac{L}{v_2}.$$

(72)

The range of applicability of our result (68) is limited by the conditions $\Delta\mu \ll v_i/L_\alpha$, $\alpha = U, D$. Outside of this range, the dependence of the visibility on the bias is nonmonotonic because of charging effects, as has been observed in the experiments.[27–30] Moreover, behavior (68) is valid only if $\Delta\mu > T$. For typical experiments[27–30] this implies that $1~\mu\mathrm{V} < \Delta\mu < 10~\mu\mathrm{V}$. We conclude that it would not be easy, but possible, in principle, to extract the exponents of the power-law behavior in Eq. (68).

To summarize, in contrast to theoretical works where *ad hoc* Klein factors are used,[24] we predict periods of AB oscillations larger than Φ_0 (for a discussion of Klein factors see Appendix C). The easiest way to experimentally detect larger periods is to compare periodicities in the weak tunneling and in the weak backscattering regimes. Equations (68) and (70) are the central results of our paper. They can be used to discriminate between different effective models. Namely, they can be fitted by measuring the current through an MZ interferometer as a function of the magnetic flux Φ and of the bias $\Delta\mu$. Evaluating the Fourier transform with respect to Φ, one can investigate the scaling in $\Delta\mu$ of different harmonics corresponding to contributions of the most relevant excitations for any charge Q_{em}. To identify the correct model, one must compare the experimentally measured scaling dimensions Δ with those in the table of Sec. IV. Once the correct model (i.e., its K matrix) is identified, one may use the temperature dependence (70) as an independent check of the theory.

VII. CONCLUSION

In the last decade, several proposals for experimental tests of the physics at a QH edge have been made. They are based on measurements of the electric charge, the statistical phases, and the scaling dimensions of quasiparticles. Some of them have been realized and have shed light on the properties of fractional QH edges. However, some experiments have brought up open questions. For instance, in the experiment,[12] the I-V curve has shown a perfect power-law behavior. However, the measured exponents, which are thought to be proportional to the scaling dimensions of the quasiparticle operators, have turned out to be different from those predicted by theory. Thus, MZ interferometers, which have already shown several interesting features, may be considered to be promising tools for probing the properties of the QH edge.

In this paper, we have reviewed the construction of a low-energy theory[8,9] of fractional QH edges based on anomaly cancellation. We have shown that for $\nu = 1/m$, where m is an odd integer, it can be described by a hydrodynamical model, while other filing factors require the introduction of several edge channels [Eq. (22)]. Quasiparticle operators in each model are found to be indexed by vectors in the dual of an odd integral lattice.[8] Their charges and statistical phases are given by Eqs. (36) and (37). We have illustrated the classification of effective models with the example of fluids with filling fraction $\nu = 2/m$ and, in particular, with $\nu = 2/3$. We have shown that, for $\nu = 2/3$, there are at least four inequivalent models satisfying all physical conditions and having the smallest possible number of fields. It is important to note that, in every effective model, the minimal fractional charge is $1/3$.

For models with two fields, we have shown that Coulomb interactions lead to universal values of electromagnetic couplings. This universality allowed us to evaluate the scaling dimensions of quasiparticles [see Eq. (42)], with the result given in Eq. (48). We have calculated the AB-oscillating contribution to the current through an MZ interferometer at low and high temperatures [Eqs. (68) and (70)] and shown that the Fourier spectrum of the current as a function of the flux can be used to extract the scaling dimensions of quasiparticle operators. This, in turn, leads to the possibility to discriminate between different effective models.

Our method to identify the correct model can be applied to fluids with arbitrary filling fractions and can be summarized as follows:

(i) First, for a given filling fraction ν, one should find solutions of Eq. (32) for K matrices, up to equivalence, as described in Eq. (38). In other words, one must identify the effective models satisfying the physical requirements formulated in Sec. II. The most interesting solutions are those with the smallest possible number of fields and minimal statistical phases of electron field operators.

(ii) Second, using Eqs. (37) and (42), one should calculate the spectra of charges and scaling dimensions for every model.

(iii) Finally, one should attempt to measure the $\Delta\mu$ scaling of the Fourier components of the current trough an MZ interferometer and compare it with theoretical predictions in order to identify a correct model.

An important aspect of our theory is that it predicts AB oscillations with quasiparticle periodicity in the gate modulated magnetic flux, i.e., with periods equal to several electronic periods. This periodicity allows one to separate the contributions of different excitations to the current. In the context of our theory, the quasiparticle periodicity is related to our choice of a tunneling Hamiltonian, which is different from the one in Refs. 24 and 26 and leads to a noncommutativity of tunneling Hamiltonians at different spatial points. This noncommutativity originates from the topological character of quasiparticle excitations in a fractional QH state and is a consequence of open boundary conditions specific to the MZ interferometer.

We think that the noncommutativity of tunneling Hamiltonians calls for additional theoretical analysis and, possibly,

for experimental tests. A theoretical analysis of this problem should include a concrete model of Ohmic contacts, which may influence the physics of processes in an MZ interferometer. It is also interesting to generalize our analysis to fractions, such as $\nu=5/2$, which are possibly described by non-Abelian QH states, and to the case of FP interferometers, where new physics may emerge.

APPENDIX A: CALCULATION OF SCALING DIMENSIONS

Using expression (40) for δ_i, we calculate the total scaling dimension Δ. As it has already been mentioned, in the general (nonchiral) case, the scaling dimension is a function of the full matrix q. Therefore, apart from the matrix K, it depends only on one additional variable, which can be fixed by choosing the Hamiltonian. We are interested in a matrix K of the following form:

$$K = \begin{pmatrix} a & b \\ b & a \end{pmatrix}. \tag{A1}$$

The connection between matrices K and q in the nonchiral case is $K=q\sigma q^T$. Therefore, we can introduce the following parametrization of the matrix q:

$$q/\sqrt{a} = \begin{pmatrix} \cosh \vartheta_1 & \sinh \vartheta_1 \\ \cosh \vartheta_2 & \sinh \vartheta_2 \end{pmatrix}, \tag{A2}$$

where $\cosh(\vartheta_2-\vartheta_1)=b/a$. Although the case $a<0$ requires a different parametrization, it leads to the same result.

The evaluation of the scaling dimension $\Delta(\mathbf{n})=\mathbf{n}(qq^T)^{-1}\mathbf{n}$ requires to invert the matrix,

$$qq^T = a \begin{pmatrix} \cosh 2\vartheta_1 & \cosh(\vartheta_1+\vartheta_2) \\ \cosh(\vartheta_1+\vartheta_2) & \cosh 2\vartheta_2 \end{pmatrix}. \tag{A3}$$

For convenience, we introduce the angle $\vartheta_+=\vartheta_1+\vartheta_2$ which takes arbitrary values and the angle $\vartheta_-=\vartheta_1-\vartheta_2$ which is fixed by the condition

$$\cosh \vartheta_- = b/a. \tag{A4}$$

Inverting the matrix qq^T [see Eq. (A3)], we find the following expression for the scaling dimensions:

$$\Delta(\mathbf{n}) = \frac{1}{b^2-a^2} \begin{pmatrix} n_1 \\ n_2 \end{pmatrix}^T \begin{pmatrix} A_- & B \\ B & A_+ \end{pmatrix} \begin{pmatrix} n_1 \\ n_2 \end{pmatrix}, \tag{A5}$$

where

$$A_\pm = b \cosh \vartheta_+ \pm \sqrt{b^2-a^2}\sinh \vartheta_+,$$

$$B = -a \cosh \vartheta_+.$$

We see that Δ indeed depends on the additional free parameter, the angle ϑ_+.

If we assume that the strong long-range Coulomb interaction is a dominant contribution to the Hamiltonian, then we may approximate $q_{11}=q_{12}$, or equivalently, $\vartheta_2=-\vartheta_1$. This condition leads to $\cosh \vartheta_+=1$ and $\sinh \vartheta_+=0$, so that the expression for the scaling dimension simplifies

$$\Delta(\mathbf{n}) = \frac{1}{b^2-a^2} \begin{pmatrix} n_1 \\ n_2 \end{pmatrix}^T \begin{pmatrix} b & -a \\ -a & b \end{pmatrix} \begin{pmatrix} n_1 \\ n_2 \end{pmatrix}. \tag{A6}$$

Calculating the product, we arrive at the final result [Eq. (48)].

Next, we evaluate the exponents δ_1 and δ_2. In the chiral case, which we consider as an example, $K=qq^T$, and the following parametrization is required:

$$q/\sqrt{a} = \begin{pmatrix} \cos \vartheta_1 & \sin \vartheta_1 \\ \cos \vartheta_2 & \sin \vartheta_2 \end{pmatrix} \tag{A7}$$

with the condition that $\cos(\vartheta_2-\vartheta_1)=b/a$. Then, using definition (40), we find

$$\delta_1(\mathbf{n}) = \frac{a}{a^2-b^2}(n_1 \cos \vartheta_1 - n_2 \cos \vartheta_2)^2, \tag{A8}$$

$$\delta_2(\mathbf{n}) = \frac{a}{a^2-b^2}(n_1 \sin \vartheta_1 - n_2 \sin \vartheta_2)^2. \tag{A9}$$

Thus, we see that by measuring the exponents δ_1 and δ_2 one can, in principle, extract the parameter ϑ_+. However, we stress again that, for strong Coulomb interaction, $\vartheta_+=0$. In this case, expressions for exponents simplify. Namely, taking into account that $a+b=2/\nu$, we find that

$$\delta_1(\mathbf{n}) = \frac{(n_1-n_2)^2}{2(a-b)}, \quad \delta_2(\mathbf{n}) = \frac{\nu}{4}(n_1+n_2)^2. \tag{A10}$$

In the nonchiral case, analogous calculations lead to similar expressions

$$\delta_1(\mathbf{n}) = \frac{(n_1-n_2)^2}{2(b-a)}, \quad \delta_2(\mathbf{n}) = \frac{\nu}{4}(n_1+n_2)^2. \tag{A11}$$

APPENDIX B: CORRELATION FUNCTION AT FINITE TEMPERATURE AND ASYMPTOTICS OF TUNNELING CURRENT

Using the Gaussian character of the edge fields ϕ_i, the correlation functions for the operators $\psi_{\mathbf{n}}=\exp[i\Sigma_j p_j(\mathbf{n})\phi_j]$ may be written in the following form:

$$i\langle \psi_{\mathbf{n}}^\dagger(x,t)\psi_{\mathbf{n}}(0,0)\rangle = e^{i\varphi_0}K_{\mathbf{n}}(x,t), \tag{B1}$$

where the first factor is the zero-mode contribution given by Eq. (67), while the function $K_{\mathbf{n}}$ is the fluctuation part,

$$\ln[K_{\mathbf{n}}(x,t)] = \sum_{ij} p_i(\mathbf{n})p_j(\mathbf{n})\langle [\phi_i(x,t)-\phi_i(0,0)]\phi_j(0,0)\rangle. \tag{B2}$$

Introducing the notation $X_j \equiv x+\sigma_j v_j t$, we express fields in terms of creation and annihilation operators,

$$\phi_j(x,t) = i\sum_k \sqrt{\frac{2\pi}{Wk}}[a_j(k)e^{ikX_j} + a_j^\dagger(k)e^{-ikX_j}], \quad \text{(B3)}$$

where W is the system size. Substituting this expression into Eq. (B2), we obtain

$$\ln[K_{\mathbf{n}}] = \sum_j p_j^2(\mathbf{n})\int_0^\Lambda \frac{dk}{k}\{f_j(k)(e^{-ikX_j} - 1)$$
$$+ [1 + f_j(k)](e^{ikX_j} - 1)\}, \quad \text{(B4)}$$

where $f_j(k) = [\exp(\beta v_j k) - 1]^{-1}$ are the boson occupation numbers and Λ is an ultraviolet cutoff.

The best way to proceed is to expand the occupation numbers in Boltzmann factors, $f_j(k) = \sum_{m=1}^\infty \exp(-\beta v_j mk)$, and integrate each term separately. This gives

$$\ln[K_{\mathbf{n}}] = -\sum_j p_j^2(\mathbf{n})\sum_{m=-\infty}^\infty \ln[\Lambda(i\beta v_j m - X_j)]. \quad \text{(B5)}$$

Combining this expression with Eq. (B1), we finally arrive at the following result:

$$i\langle\psi_{\mathbf{n}}^\dagger(x,t)\psi_{\mathbf{n}}(0,0)\rangle \propto e^{i\varphi_0}\prod_i\left[\frac{v_i}{\pi T}\sinh\left(\pi\frac{TX_i}{v_i}\right)\right]^{-\delta_i(\mathbf{n})}. \quad \text{(B6)}$$

The scaling exponents δ_i are calculated in Appendix A.

Next, we use high-temperature limit (69) of the correlation function (B6) to calculate the high-temperature asymptotics of the tunneling current. Substituting the correlation function (69) into Eq. (65), we obtain the following expression:

$$I_\Phi \propto \mathrm{Re}\int_{-\infty}^{+\infty}dt e^{i\Delta\mu t}T^{2\Delta(\mathbf{n})}\exp\left(-\pi T\sum_{i,\alpha}|t + \sigma_i L_\alpha/v_i|\delta_i(\mathbf{n})\right). \quad \text{(B7)}$$

In the limit $T \gg \Delta\mu$, we approximate $e^{i\Delta\mu t} \simeq 1 + i\Delta\mu t$, where only the second term makes a nonzero contribution,

$$I_\Phi \propto \Delta\mu T^{2\Delta(\mathbf{n})}\int_{-\infty}^{+\infty}dt\, t\exp\left(-\pi T\sum_{i,\alpha}|t + \sigma_i L_\alpha/v_i|\delta_i(\mathbf{n})\right). \quad \text{(B8)}$$

In the high-temperature limit, the largest contribution to this integral comes from a small region around one of the points $t = -\sigma_i L_\alpha/v_i$, where the argument of the exponential function acquires the smallest absolute value. Then the time integral can be estimated as

$$\int_{-\infty}^{+\infty}dt\, t\exp\left(-\pi T\sum_{i,\alpha}|t + \sigma_i L_\alpha/v_i|\delta_i(\mathbf{n})\right) \propto T^{-1}e^{-\pi T/T_0(\mathbf{n})}, \quad \text{(B9)}$$

where the energy scale $T_0(\mathbf{n})$ is given by Eq. (71). Using this result, we finally arrive at the asymptotics [Eq. (70)] of the oscillating part of the current.

APPENDIX C: TUNNELING HAMILTONIAN

In this appendix, we discuss two important questions concerning the form of tunneling Hamiltonians. The first question is whether one needs to introduce Klein factors[22] to ensure commutativity of the tunneling Hamiltonians at spatially separated points. We argue that the correct choice of the tunneling Hamiltonian generally leads to AB oscillations in the quasiparticle current. The second question is about the value of the AB phase shift that should be included in tunneling amplitudes.

1. Noncommutativity and Klein factors

For simplicity let us consider the case of filling factor $\nu = 1/m$, where only one channel at each edge of the MZ interferometer is present. Tunneling of Laughlin quasiparticles is described by the Hamiltonian $\mathcal{H}_L + \mathcal{H}_R$, where

$$\mathcal{H}_\ell = t_\ell\psi_U^\dagger(x_\ell)\psi_D(x_\ell) + t_\ell^*\psi_D^\dagger(x_\ell)\psi_U(x_\ell), \quad \ell = L,R \quad \text{(C1)}$$

are the contributions at two spatially separated points x_L and x_R. It is interesting to calculate the commutator of $\mathcal{H}_L$ and $\mathcal{H}_R$. For this purpose, we first have to find the commutation relations for quasiparticle operators in a system with two edges.

We remind the reader that only local excitations may tunnel at QPCs. One of the conditions of locality reads

$$[\partial_x\phi_U, \psi_D] = 0, \quad [\partial_x\phi_D, \psi_U] = 0, \quad \text{(C2)}$$

which means that a quasiparticle at one edge does not create a charge density at the other edge. This condition implies that $[\psi_U, \psi_D] = 0$. On the other hand, for quasiparticle operators at the same edge, in the case of open boundary conditions, we have that

$$\psi_\alpha(x)\psi_\alpha(x') = e^{(i\pi/m)\mathrm{sgn}(x'-x)}\psi_\alpha(x')\psi_\alpha(x), \quad \text{(C3)}$$

where $\alpha = U, D$ and the coordinate x starts at the Ohmic contact and increases in the direction of the chirality of the corresponding channel.

The sign of the statistical phase in this expression is determined by the sign of the right-hand side of Eq. (12) and depends on the chirality of the channel. Assuming $x_R > x_L$ (see Fig. 7), we arrive at the following result:

$$\psi_U^\dagger(x_L)\psi_D(x_L)\psi_U^\dagger(x_R)\psi_D(x_R)$$
$$= e^{2\pi i/m}\psi_U^\dagger(x_R)\psi_D(x_R)\psi_U^\dagger(x_L)\psi_D(x_L). \quad \text{(C4)}$$

Thus, we conclude that for the tunneling Hamiltonians defined in Eq. (C1), $[\mathcal{H}_L, \mathcal{H}_R] \neq 0$. Note that this is not the case for a Fabry-Pérot-type interferometer, where the order of tunneling points with respect to chirality is different on different arms. Therefore, contributions to the statistical phase from inner and outer edges cancel, and the Hamiltonians $\mathcal{H}_L$ and $\mathcal{H}_R$ commute.

There is a useful geometrical illustration of the commutation relations discussed above. It is a well known fact about the Chern-Simons effective theory that the quasiparticle operator can be represented as a Wilson line.[49] According to the boundary conditions for the excitations in the MZ interfer-
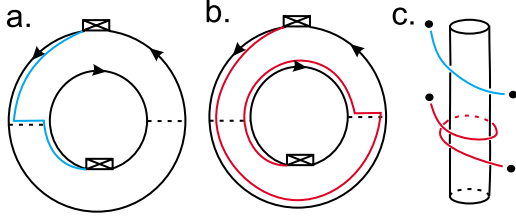
FIG. 8. (Color online) The Mach-Zehnder interferometer and Wilson lines are schematically shown. Tunneling Hamiltonians may be expressed in terms of integrals along the lines between Ohmic contacts [see Eq. (C5)]. Panel a: The Wilson line (drawn in blue) corresponds to tunneling at the left QPC, described by the Hamiltonian $\mathcal{H}_L$. Panel b: The Wilson line (drawn in red) for the Hamiltonian $\mathcal{H}_R$. Panel c: "Time-expanded" representation of the product $\mathcal{H}_R \mathcal{H}_L$. We see that the two lines cannot be "topologically exchanged," which means that the two Hamiltonians $\mathcal{H}_L$ and $\mathcal{H}_R$ do not commute.

ometer, we choose the Ohmic contacts as end points of Wilson lines (see the discussion in Appendix D). Thus, the tunneling Hamiltonians are given by Wilson lines going from one Ohmic contact to the other,

$$\mathcal{H}_\ell = t_\ell \exp\left[\frac{i}{\sqrt{m}} \int_{\gamma_\ell} dr^\mu b_\mu\right] + t_\ell^* \exp\left[\frac{i}{\sqrt{m}} \int_{-\gamma_\ell} dr^\mu b_\mu\right],$$
(C5)

where b_μ is the Chern-Simons field and γ_ℓ is the line going from the upper Ohmic contact to the lower one through the ℓth QPC [see Figs. 8(a) and 8(b)].[50] The product of these operators, $\mathcal{H}_R \mathcal{H}_L$, is represented by the configuration of Wilson lines shown schematically in Fig. 8(c). On the other hand, the permutation $\mathcal{H}_L \mathcal{H}_R$ of these operators may be represented by the lines oppositely ordered in time. According to Chern-Simons theory the corresponding braidings again yield result (C4). Interestingly, for a FP interferometer, the corresponding braidings are trivial (see Fig. 9); therefore, the tunneling Hamiltonians commute.

Noncommutativity of tunneling Hamiltonians has often been claimed in the literature to be unphysical. It has therefore been proposed to use Klein factors to ensure their commutativity. To clarify the nature of Klein factors, we consider
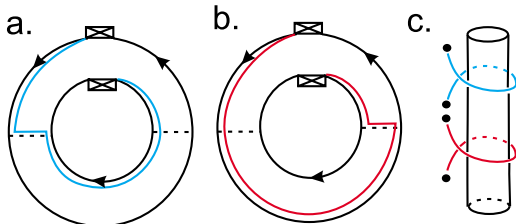

FIG. 9. (Color online) The Fabry-Pérot interferometer and Wilson lines are schematically shown. Panel a: Wilson line (drawn in blue), which represents the Hamiltonian $\mathcal{H}_L$, differs from the one for the MZ interferometer. Panel b: Wilson line (drawn in red) for the Hamiltonian $\mathcal{H}_R$. Panel c: Time-expanded representation of two Wilson lines. One can see that the lines are topologically identical, therefore Hamiltonians $\mathcal{H}_L$ and $\mathcal{H}_R$ commute.

for a moment the boundary conditions which correspond to a closed geometry. In this case the quasiparticle operators $\psi_\alpha = e^{(i/\sqrt{m})\phi_\alpha(x)}$ are m-fold multivalued operators. This is because the field $\phi_\alpha(x)$ is, in fact, an integral of the density ρ_α over a closed contour that can have different numbers of winding, $\kappa = 0, 1, \ldots, m-1$. Hence, we can write

$$\phi_\alpha(x) = \phi_\alpha + 2\pi(x + \kappa W_\alpha)\pi_\alpha + \text{osc.}, \quad \alpha = U, D, \quad \text{(C6)}$$

where ϕ_α and π_α are the zero modes and W_α is the length of the boundary α.

We stress that only *relative* branch numbers are physically observable. Indeed, the two zero modes π_α, where $\alpha = U, D$, are quantized as $W_\alpha \pi_\alpha = N_\alpha / \sqrt{m}$. However, any closed electronic system contains an integer number, N, of electrons, which imposes the following constraint on the total charge operator: $(W_U \pi_U + W_D \pi_D)/\sqrt{m} = N$. This limitation on the eigenvalues of the operators π_α, which any physically allowed state should satisfy, leads to the fact that

$$F \equiv e^{(2\pi i/\sqrt{m})W_U \pi_U} = e^{-(2\pi i/\sqrt{m})W_D \pi_D}. \quad \text{(C7)}$$

We use the winding number κ as an additional index that denotes the quasiparticle branch, $\psi_{\alpha,\kappa} = \psi_\alpha F^\kappa$. Here ψ_α stands for the case, where $\kappa = 0$, i.e., for the branch that starts from one of the Ohmic contacts. In the language of Wilson lines, every branch is given by a line with the corresponding number of windings.

If several branches are present, then one should take into account all possible processes in the tunneling Hamiltonian including those that change the quasiparticle branch number. Therefore, in general, the tunneling Hamiltonian can be written as

$$\mathcal{H}_\ell = \sum_{\kappa'} t_{\ell,\kappa'} \psi_{D,\kappa}^\dagger(x_\ell) \psi_{U,\kappa+\kappa'}(x_\ell) + \text{H.c.} \quad \text{(C8)}$$

The commutation relations for quasiparticle operators [Eq. (C3)] are easily generalized,

$$\psi_\kappa(x)\psi_{\kappa'}(x') = e^{(2i\pi/m)(\kappa-\kappa')}e^{(i\pi/m)\text{sgn}(x'-x)}\psi_{\kappa'}(x')\psi_\kappa(x),$$
(C9)

and we arrive at the important conclusion that, in general, Hamiltonians (C8), taken at different spatial points, do not commute.

In order to put our discussion into the context of previous work, we rewrite Hamiltonian (C8) in a slightly different form,

$$\mathcal{H}_\ell = \sum_\kappa t_{\ell,\kappa} F^\kappa \psi_D^\dagger(x_\ell)\psi_U(x_\ell) + \text{H.c.}, \quad \text{(C10)}$$

where the operator F introduced earlier obviously plays the role of a Klein factor. Interestingly, in the specific case when only the amplitudes $t_{L,1}$ and $t_{R,0}$ are nonzero, tunneling Hamiltonians (C10) do commute at different spatial points. Moreover, in the language of Wilson lines the multiplication of the tunneling Hamiltonian with the Klein factor F is equivalent to adding a loop to the corresponding Wilson line, so that it goes all the way around the interferometer. It is easy to see that adding such a loop to the blue line in Fig. 8 makes it topologically equivalent to the red line. Therefore,

the Hamiltonians, after such manipulation, indeed commute.

Here we have to admit that the Klein factors introduced earlier in the literature are usually supposed to commute with the quasiparticle operators ψ_α (see, for instance, Refs. 22 and 25). In other words, they act on some additional Hilbert space. This situation, however, is not satisfactory because it contradicts the very well known aspect of the QHE that there exists a gap for excitations in the bulk, and the only degrees of freedom available are the edge excitations $\phi_\alpha(x)$, including zero modes ϕ_α and π_α. Therefore, we think that Klein factors should be expressed in terms of the same modes as the operators ψ_α (see, e.g., Ref. 51). On the other hand, choosing specific Hamiltonians that commute does not appear to be physical and needs, to say the least, additional justification. Moreover, it is important that Klein factors may be introduced only in a system with a closed geometry, where multivalued excitations may exist. The strong coupling to Ohmic contacts, as in the case of an MZ interferometer considered in this paper, requires open boundary conditions. Therefore, we insist that our form (C1) of the tunneling Hamiltonian is correct and use it in Sec. VI for calculations.

Our next remark concerns the statement made in the literature[24,26,52,53] that it is impossible to observe a coherent part of the quasiparticle current. It has been claimed that several degeneracies are present in a system which lead to strong dephasing via two mechanisms. Within our approach the first mechanism[24] can be interpreted as being based on the fact that there exists a set of quasidegenerate states which correspond to a shift of both edges.[6] One may parametrize them as following:

$$\frac{W_U \pi_U}{\sqrt{m}} = N + \frac{l}{m}, \qquad \frac{W_D \pi_D}{\sqrt{m}} = N - \frac{l}{m}, \qquad \text{(C11)}$$

where $l = 0, \ldots, m-1$. We denote these states with $|l\rangle$ and write $|l+1\rangle = e^{i(\phi_U + \phi_D)/\sqrt{m}}|l\rangle$. The density matrix for the interferometer, with the QH edges in an equilibrium state, can be written as

$$\rho_0 = \sum_{l=0}^{m-1} r_l |l\rangle\langle l|. \qquad \text{(C12)}$$

The coherent part of the current generated by tunneling Hamiltonian (C8) and averaged with the density matrix (C12) reads

$$I_{LR} \propto \sum_l \sum_{\kappa,\kappa'} r_l t_{L,\kappa} t^*_{R,\kappa'} \langle l| F^{\kappa-\kappa'}|l\rangle. \qquad \text{(C13)}$$

In our paper we use tunneling Hamiltonian (C1) with $\kappa = \kappa'$. Therefore, the summation over the quantum number l is trivial, $\Sigma_l r_l = 1$, and does not lead to any physical effect. In contrast, using additional Klein factors[24] implies that $\kappa - \kappa' = 1$. Thus, in Eq. (C13), the contribution from every shifted state $|l\rangle$ acquires the phase factor $\langle l| F|l\rangle = e^{2\pi i l/m}$. Law *et al.*[24] further assumed equal population $r_l = 1/m$, so that, after summation over l, the coherent part of the quasiparticle current vanishes.

In the argument sketched above, in addition to the specific choice $\kappa - \kappa' = 1$ that has been addressed earlier, the assumption of the degeneracy of states $|l\rangle$, or equivalently, the high-temperature limit $r_l = 1/m$, is of crucial importance. We note, however, that shift (C11) leads to charging of the edges and the corresponding energy is not small. The experiments[27–30] have been done in the regime where the temperature and the bias are smaller than this charging energy, and we do not see any difficulties, in principle, to achieve such a regime in the fractional QHE case.

A second possible mechanism of dephasing is described in Ref. 52. An additional Berry phase shift between two tunneling paths may appear if some number l of localized quasiparticles are present in the bulk. In this case the coherent contribution to the tunneling current acquires the phase factor $e^{2\pi i l/m}$, which is similar to the one encountered in the first mechanism of dephasing discussed above. If the number, l, of quasiparticles fluctuates, then the coherent part of the quasiparticle current may vanish,

$$I_{LR} \propto \sum_l e^{2\pi i l/m} \to 0,$$

as a result of averaging over these fluctuations. We would like to stress that this mechanism may be avoided either by reducing the temperature, so that the activation of spontaneous phase slips is slow, or by using a high-quality sample. For instance, in the integer QHE case such telegraph processes have indeed been observed in the experiment[30] and then reduced by tuning the system's parameters.

To conclude, we recall that the MZ interferometer, being a system that is strongly coupled to Ohmic contacts, requires open boundary conditions. This leads to the noncommutativity of tunneling Hamiltonians taken at different spatial points. We think that the noncommutativity of spatially separated operators naturally follows from the topological character of the effective theory, according to which the quasiparticles are not completely local objects, because they have "tails" in form of Wilson lines. Moreover, the nonlocality in the effective theory does not contradict the local character of the underlying microscopic theory which does not necessary manifest itself in the low-energy limit. The Klein factors, which have been introduced in earlier papers to ensure the commutativity of tunneling Hamiltonians, require, in fact, closed boundary conditions and are therefore not applicable to MZ interferometers. Moreover, we have shown that even when Klein factors may be used, they cannot guarantee the commutativity of tunneling Hamiltonians in general, while the specific choice proposed in Refs. 22 and 24 needs further justification. Finally, we remark that the strong suppression of the phase coherence suggested in Refs. 24 and 52 is not a fundamental property of the fractional QHE and may be avoided in future experiments at sufficiently low temperatures.

2. Periodicity in magnetic flux and modulation gate voltage

The purpose of this discussion is to clarify the origin of the quasiparticle periodicity in physical observables. Let us first analyze the dependence of the energies of the zero
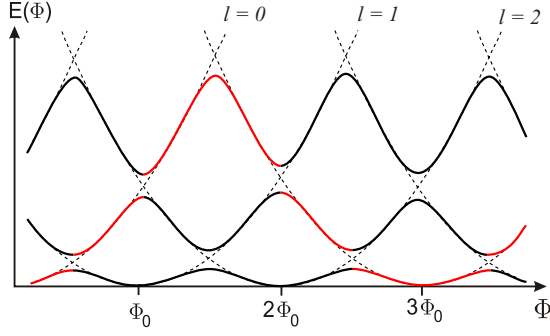
FIG. 10. (Color online) The energy spectrum of a QH fluid at $\nu=1/3$ in a Corbino disk is schematically shown. The dashed lines show the Coulomb charging energy of an isolated QH fluid as a function of the magnetic flux Φ threading the Corbino disk. Different branches correspond to different numbers of quasiparticles at the edges. In the presence of interedge quasiparticle tunneling and for weak coupling to metallic reservoirs, an energy gap opens at the degeneracy points, where different branches intersect. If the flux varies adiabatically, the QH fluid follows the ground state, so that the energy is a periodic function of the flux with the electronic period Φ_0. If the variation of the flux is relatively fast (quasiparticle tunneling is weak), the QH fluid follows the "electronic" branch (shown in red) along the lines $l=0$, $l=3$, etc., so that the number of electrons at the edge changes by one. In this case the energy oscillates with the quasiparticle period $3\Phi_0$.

modes eigenstates $|l\rangle$ (see Appendix C 1) of a QH fluid at $\nu=1/m$ on the singular magnetic flux Φ threading the Corbino disk. This problem has been considered by Thouless and Gefen in Ref. 54. Following their argument, we note that the main contribution to the energy comes from Coulomb interactions. Therefore, under variation of the flux Φ, the energies of zero modes eigenstates of a QH fluid, isolated inside a Corbino disk, follow the branches with a fixed number of electrons. However, if the Corbino disk is weakly coupled to metallic reservoirs, the number of electrons in the QH fluid is not conserved. Therefore, if the ground state energy initially grows with the flux Φ, it then switches to another branch by changing the number of electrons by 1 and starts to decrease with the flux. This behavior (shown by the red line in Fig. 10) repeats periodically with a period equal to $m\Phi_0$.

The electronic periodicity is restored if one takes into account the possibility of quasiparticle tunneling between the inner and outer edges of the Corbino disk. Such a perturbation mixes the states $|l\rangle$, with $l=0,\ldots,m-1$, and opens a gap at the degeneracy points (see Fig. 10). As a result, under an adiabatic variation of the magnetic flux, the QH fluid will follow the lowest energy state with the electronic period Φ_0.

Far away from equilibrium, when a potential difference is applied to metallic reservoirs and a charge current flows through an MZ interferometer, the physical situation is generally more complicated. However, one can still rely on the effective theory by taking into account the described above dependence of the energy of zero modes on the magnetic flux and writing the Hamiltonian as

$$\mathcal{H} = \sum_{s=U,D} \frac{v_s}{4\pi} \int dx \left(\partial_x \phi_s + \frac{2\pi}{W_s\sqrt{m}} \frac{\Phi}{\Phi_0} \right)^2. \quad \text{(C14)}$$

We stress that the insertion of the singular flux does not affect the AB phase. This follows form the fact that there are two contributions to the integral $\delta\varphi_{AB}=(1/\sqrt{m})\int_\gamma dr^\mu \delta b_\mu$ over the MZ contour γ. One contribution arises from the change in the field b_μ due to the variation of the external field A_μ, as follows from relation (D7). The second contribution comes from the variation of the total charge inside the MZ contour, repelled by the singular flux, according to relation (D1). These two effects cancel each other exactly, which can be viewed as a result of screening of the external field A_μ by the QH system.

To determine the current through the interferometer the averaging in the linear-response formula (65) must be done with respect to the equilibrium density matrix $\rho_0=e^{-\beta\mathcal{H}}/Z_0$. In the thermodynamic limit, the fields $\partial_x\phi_s$ can be shifted when performing the averaging so as to eliminate the dependence on the magnetic flux from Hamiltonian (C14). This implies that the only physical consequence of the insertion of the singular magnetic flux in a finite size Corbino disk is the Coulomb blockade effect which has an electronic periodicity. However, this effect is absent in MZ interferometers due to the strong coupling to Ohmic contacts.

The modulation of the AB phase via the insertion of a pointlike flux is an idealization. In a typical experiment, the magnetic field can be changed only uniformly. In this case the phase acquired by a quasiparticle is no longer a topological number and may depend, e.g., on the processes in Ohmic contacts in a complicated way. Therefore, it appears to be more appropriate to investigate the periodicity of AB oscillations by changing the modulation gate voltage instead of changing the magnetic field.

A gate voltage applied at the edge of a QH liquid leads to the displacement $y(x)$ of the edge at the point x. This displacement may be described as an accumulation of background 1D charge densities, $\delta\rho_i(x)=\sigma_i Q_i^2 y(x)/2\pi l_B^2$, in the edge channels. In the presence of these densities, the fields ϕ_i are redefined as $\partial\phi_i \to \partial\phi_i + \sigma_i Q_i y(x)/l_B^2$. As a consequence, the correlation function $\langle\psi^\dagger(x,t)\psi(0,0)\rangle$ of an excitation $\psi=e^{ip_i\phi_i}$ acquires a phase shift $\delta\varphi_0 = \sigma_i p_i Q_i \int_0^x dx' y(x')/l_B^2$. This phase shift is proportional to the charge of the quasiparticle, $Q_{em}(\mathbf{n})=\Sigma_i \sigma_i p_i Q_i$, and to the area of the deformation, $S=\int_0^x dx' y(x')$. Therefore, the phase shift may be interpreted as an AB phase,

$$\delta\varphi_0(\mathbf{n}) = Q_{em}(\mathbf{n}) \cdot S/l_B^2 = 2\pi Q_{em}(\mathbf{n}) \frac{\delta\Phi}{\Phi_0}, \quad \text{(C15)}$$

where $\delta\Phi$ is the variation of the magnetic flux through the closed path of the MZ interferometer, resulting from the deformation. For simplicity of notations, additional phase (C15) is included in the tunneling amplitudes in Eq. (59).

To conclude, in our model, the periodicity of AB oscillations in the average current is determined by the charges of quasiparticles that tunnel. To verify this prediction, one should compare the periodicity in the weak tunneling regime,

where only electron tunneling is possible, with the one in the weak backscattering regime, where the tunneling of quasiparticles is most relevant.

APPENDIX D: CHERN-SIMONS THEORY AND ILLUSTRATION OF HOLOGRAPHY

In this appendix we illustrate the holographic principle by constructing the bulk effective models and showing that they determine the minimal edge models discussed in Sec. III. We assume that the edge currents originate as deformations of incompressible fluids. These fluids are described by a family of separately conserved bulk currents, $j_{i\mu}$, with $\partial_\mu j_i^\mu = 0$. We solve the continuity equations by introducing potentials $b_{i\mu}$,

$$j_{i\mu} = \frac{1}{2\pi} \epsilon_{\mu\nu\lambda} \partial^\nu b_i^\lambda, \tag{D1}$$

where the Einstein summation convention is assumed. The currents are invariant under the gauge transformations $b_{i\mu} \to b_{i\mu} + \partial_\mu f_i$. By counting dimensions, it is easy to see that the gauge-invariant action for these potentials,

$$S_{\text{bulk}}[b_i] = (1/4\pi)\sum_i \sigma_i \int_D d^3r \epsilon_{\mu\nu\lambda} b_i^\mu \partial^\nu b_i^\lambda, \tag{D2}$$

has zero dimension, while all other possible terms have *lower* dimensions, i.e., are *irrelevant* at low energies. For example, the Maxwell-like action has dimension -1.

The total electric current can be written as a linear combination of incompressible currents $j_{\text{em}}^\mu = \sum_i Q_i j_i^\mu$. Hence, the term in the action describing the interaction with an external electromagnetic field is

$$S_{\text{int}}[b_i, A] = \int_D d^3r A_\mu j_{\text{em}}^\mu = (1/2\pi)\sum_i \int_D d^3r A_\mu Q_i \epsilon^{\mu\nu\lambda} \partial_\nu b_{i\lambda}. \tag{D3}$$

Integrating out the fields $b_{i\mu}$, we arrive at an effective action for the electromagnetic field in the Chern-Simons form,

$$S_{\text{eff}}[A] = (1/4\pi)\sum_i \sigma_i Q_i^2 \int_D d^3r \epsilon^{\mu\nu\lambda} A_\mu \partial_\nu A_\lambda. \tag{D4}$$

Comparing this result to Eq. (23), we conclude that the constraint on the coupling constants Q_i is the same as in the edge theory, namely, $\sum_i \sigma_i Q_i^2 = \nu$.

Action (D2) appears in the context of topological theory, where excitations are given by Wilson lines.[49] For instance, a general local excitation at the point r may be written as

$$\psi_q(r) = \exp\left(i\sum_j q_j \int_{r_0}^r dr^\mu b_{j\mu} \right). \tag{D5}$$

The statistical phase of two excitations of type (D5) is given by braiding of the corresponding Wilson lines.[49] Considering two excitations labeled with q_{1j} and q_{2j} we arrive, after a simple calculation of braiding, at the following expression for the statistical phase: $\theta_{12} = \pi\sum_i \sigma_i q_{1j} q_{2j}$. It is important that this expression coincides with the one for the edge excita-
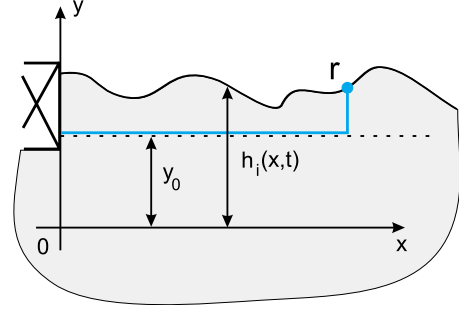

FIG. 11. (Color online) The construction of edge excitations as incompressible deformations of a QH liquid. The Wilson line (drawn in blue) starts from the Ohmic contact (drawn in white) and goes to the physical edge $y = h_i(x,t)$ of the ith QH liquid (solid line) along the auxiliary boundary at $y = y_0$ (dashed line), and ends at the point r.

tions. Moreover, if we define the charge operator as an integral over a spacelike plane $Q_{\text{em}} = (Q_i/2\pi)\int d^2r \epsilon_{\nu\lambda} \partial^\nu b_i^\lambda$, then the charge of excitation (D5) is $Q_{\text{em}} = \sum_i \sigma_i Q_i q_i$, i.e., it takes the same form as in the edge theory.

The coincidence of bulk and edge expressions for charges and statistical phases of excitations illustrates the holographic principle at work in QH systems. Indeed, it is easy to see that the whole classification of effective models at the edge applies also to the bulk. Furthermore, Fröhlich and Pedrini[55] proposed an exact mapping between edge and bulk models, assuming that the edge excitations originate from incompressible deformations of QH liquids. Below we summarize the main steps of this construction.

The key idea is to represent the insertion of an operator $\exp(i\sum_j q_j \phi_j)$ at the edge as insertion of Wilson line (D5) of the bulk theory by placing the end point r at the boundary and r_0 in the Ohmic contact. To realize this idea we choose a particular Wilson line shown in Fig. 11. Parametrizing incompressible deformations of QH liquids by the set of functions $y = h_i(x,t)$, one may introduce the boundary fields,

$$\phi_i(x,t) = \int_{y_0}^{h_i(x,t)} dy' b_{iy}(x,y',t) + \int_{x_0}^x dx' b_{ix}(x',y_0,t), \tag{D6}$$

where $y = y_0$ is the auxiliary boundary and x_0 is the coordinate of the Ohmic contact.

Integrating out the bulk fields $b_{i\mu}$, we find that[56]

$$b_{i\mu} = \sigma_i Q_i A_\mu. \tag{D7}$$

Taking the derivative of Eq. (D6) with respect to x, one obtains $\sigma_i \partial_x \phi_i = Q_i A_y(x,h_i,t)\partial_x h_i + Q_i \int_{y_0}^{h_i} dy' \partial_x A_y(x,y',t) + Q_i A_x(x,y_0,t)$. In the low-energy limit we may neglect the term proportional to $\partial_x h_i$. Then, taking into account that the magnetic field is constant $\partial_x A_y - \partial_y A_x = 1/l_B^2$, we relate the derivatives $\partial_x \phi_i$ to the edge densities[57] $\rho_i(x,t) = \sigma_i Q_i^2[h_i(x,t) - y_0]/2\pi l_B^2$,

$$\rho_i(x,t) = \frac{1}{2\pi}[Q_i\partial_x\phi_i + \sigma_i Q_i^2 A_x(x,h_i,t)]. \quad \text{(D8)}$$

This expression for the charge densities of the edge channels coincides with the one derived from action (22), provided we further assume that h_i is small in the low-energy limit and replace $A_x(x,h_i,t) \to A_x(x,y_0,t)$. In other words, we assume linear coupling to the electromagnetic field.

The continuity equations $\dot{\rho}_i + \partial_x\int_{y_0}^{h_i}j_{ix} = j_{iy}$, after the substitution of Eq. (D1), take the form

$$\frac{Q_i\dot{h}_i}{2\pi l^2} + \partial_x\int_{y_0}^{h_i}dy'[\partial_{y'}b_{it}(x,y',t) - \partial_t b_{iy}(x,y',t)]$$
$$= \partial_x b_{it}(x,y_0,t) - \partial_t b_{ix}(x,y_0,t). \quad \text{(D9)}$$

Linearizing this equation with respect to h_i, we find the equations of motion for the boundary fields $\sigma_i\partial_t D_x\phi_i = -Q_i\partial_x a_t$, where a_μ is the boundary value of the electromagnetic vector potential and $D_\mu\phi_i = \partial_\mu\phi_i + \sigma_i Q_i a_\mu$ are covariant derivatives. These equations of motion can be derived from the action

$$S \propto \sum_i \int dt dx(\sigma_i D_t\phi_i D_x\phi_i + Q_i\epsilon_{\mu\nu}a^\mu\partial^\nu\phi_i), \quad \text{(D10)}$$

which agrees with action (22) in the case $v_i = 0$. The velocities of edge modes in the above analysis are zero because we have not taken into account the confining potential and the interaction effects at the edge.

It is important to note that the bulk-edge correspondence described above does not always hold. For instance, compressible strips may be present at the edge.[14] In this case, the edge theory will contain more fields than the bulk theory. Nevertheless, bulk excitations should be always present in the edge spectrum. In the present work we only consider minimal models of the edge for the following reasons. First of all, in the case when the number of chiral fields at the edge is large, scaling dimensions of extra electrons associated with these fields are usually large,[8] i.e., these excitations are not observable in the low-energy limit. Second, nonchiral models with additional fields are likely to be unstable against disorder.[15] However, the possible relevance of models with a large number of channels deserves a separate detailed analysis.

APPENDIX E: MATHEMATICAL ASPECTS OF THE THEORY OF QH LATTICES

In this section we wish to briefly describe the QH lattice construction proposed in Refs. 8 and 55. This construction is a mathematical reformulation of physical requirements for the effective theory of a QH system discussed in Secs. II and III. It provides a method, based on using invariants of lattices, to classify physically allowed low-energy effective models of QH edge states. The main physical consequences of the lattice construction include a determination of the minimal charge of quasiparticle, of the minimal number of edge channels, for given filling factor, etc. Here we summarize the lattice construction and present the results without proof.

First, we recall that action (22) of the effective theory is parameterized by the vector of coupling constants, Q_i, introduced in Sec. III. Local excitations are represented by vertex operators, $\exp(i\Sigma_j q_j\phi_j)$, and labeled by vectors $\mathbf{q} = \{q_i\}$, so the sum of two such vectors corresponds to the product of operators. Defining the scalar product,

$$\langle\mathbf{a},\mathbf{b}\rangle = \sum_i a_i b_i \sigma_i, \quad \text{(E1)}$$

where σ_i is the chirality of ith channel, we represent electric charge (27) of an excitation corresponding to the vector $\mathbf{q}$ and statistical phase (26) of two excitations corresponding to $\mathbf{q}_1$ and $\mathbf{q}_2$ as

$$Q_{\rm em} = \langle\mathbf{Q},\mathbf{q}\rangle, \quad \theta_{12} = \pi\langle\mathbf{q}_1,\mathbf{q}_2\rangle, \quad \text{(E2)}$$

respectively.

As discussed in Sec. III, after fixing the coupling constants Q_i (i.e., fixing the action), we have to choose electronic excitations. We denote them with $\mathbf{q}_\alpha$. Multielectron excitations form an integral lattice Γ:

$$\Gamma = \{k_\alpha\mathbf{q}_\alpha | k_\alpha \in \mathbb{Z}\}. \quad \text{(E3)}$$

It has been mentioned in Sec. III B that choosing some different sets of elementary electronic excitations is equivalent to choosing different bases in the same lattice Γ. Thus, the lattice Γ describes an effective theory in a basis-independent way. The condition that the electric charge $\langle\mathbf{Q},\mathbf{q}\rangle$ of any combination of electrons $\mathbf{q} \in \Gamma$ is integer implies that the vector of couplings $\mathbf{Q}$ belongs to the dual lattice Γ^*. Thus, by choosing the lattice Γ and a vector $\mathbf{Q}$ of its dual, one selects a particular effective model.

Next, important physical constraints on the effective models discussed in Sec. II can be formulated as following:

(i) The condition of anomaly cancellation, for a given filling fraction ν, implies that $\langle\mathbf{Q},\mathbf{Q}\rangle = \nu$.

(ii) The correct charge of electronic operators is guaranteed if the greatest common divisor of the coordinates of $\mathbf{Q}$ in Γ^* is equal to 1 because this divisor is equal to the minimal value of $\langle\mathbf{Q},\mathbf{q}\rangle$ for $\mathbf{q} \in \Gamma$.

(iii) The correct statistical phase of electronic excitations is a consequence of the condition $\langle\mathbf{Q},\mathbf{q}\rangle \equiv \langle\mathbf{q},\mathbf{q}\rangle(\text{mod } 2)$, $\forall\mathbf{q} \in \Gamma$.

The spectrum of allowed local excitations follows from the requirement that the wave function of the QH state is single-valued in the presence of an excitation $\exp(i\Sigma_j p_j\phi_j)$. We mentioned in Sec. II that this condition is equivalent to having integer relative statistical phases between electrons and quasiparticles,

$$\langle\mathbf{p},\mathbf{q}_\alpha\rangle \in \mathbb{Z}. \quad \text{(E4)}$$

Thus, the lattice of allowed excitations is $\Gamma^* \supseteq \Gamma$. As we have shown in Sec. III, the scaling dimension, Δ, of the correlation function of the excitation $\mathbf{p}$ does not depend on the Hamiltonian in a purely chiral theory. It is equal to the statistical phase $\Delta = \langle\mathbf{p},\mathbf{p}\rangle$. So, for purely chiral models, the pair $(\Gamma,\mathbf{Q})$ provides complete information about the effective theory. In order to do explicit calculations, one needs to introduce a particular basis for Γ. It is, however, not trivial to verify whether two different bases generate the same lattice.

To distinguish effective models and, therefore, classify them, one needs basis-independent information about lattices. Such information is provided by *lattice invariants*.

To classify the pairs $(\Gamma, \mathbf{Q})$ satisfying the conditions discussed above, we introduce most important lattice invariants. Obvious invariants are the filling factor $\nu = n_H/d_H$, with n_H and d_H as coprime integers, and the dimension (or rank) of the lattice $N = \dim \Gamma$. One may show that, for any basis, $\{\mathbf{e}_\alpha\}$, of Γ, the determinant of the Gram matrix $\Delta_\Gamma = \det \langle \mathbf{e}_\alpha, \mathbf{e}_\beta \rangle$ is also an invariant.[58] An interesting property of this determinant is the factorization $\Delta_\Gamma = l d_H$, where l is an integer number called *level*. Moreover, one may show that, for any basis $\{\mathbf{e}^\alpha\}$ of Γ^*, the greatest common divisor $g = \gcd(Q^1, \ldots, Q^N)$ of the numbers $Q^\alpha = \Delta_\Gamma \langle \mathbf{Q}, \mathbf{e}^\alpha \rangle$ is an invariant and that $l = \lambda g$, where λ is an integer. This number λ is an important parameter often called the *charge parameter*. It determines the minimal possible electric charge of a quasiparticle,

$$e^* = \min_{\mathbf{p} \in \Gamma^*, \langle \mathbf{Q}, \mathbf{p} \rangle \neq 0} |\langle \mathbf{Q}, \mathbf{p} \rangle| = \frac{1}{\lambda d_H}. \tag{E5}$$

Finally, one introduces two further invariants, called minimal and maximal relative angular momenta. The minimal relative angular momentum is defined as

$$\ell_{\min} = \min_{\mathbf{q} \in \Gamma, \langle \mathbf{Q}, \mathbf{q} \rangle = 1} \langle \mathbf{q}, \mathbf{q} \rangle. \tag{E6}$$

Introducing the set, $B_{\mathbf{Q}}$, of all possible electronic bases, $\{\mathbf{q}_\alpha\}$, of Γ, for a given $\mathbf{Q}$ (i.e., such that $\forall \alpha : \langle \mathbf{Q}, \mathbf{q}_\alpha \rangle = 1$), one defines the maximal relative angular momentum as

$$\ell_{\max} = \min_{\{\mathbf{q}_\alpha\} \in B_{\mathbf{Q}}} (\max_\alpha \langle \mathbf{q}_\alpha, \mathbf{q}_\alpha \rangle). \tag{E7}$$

The invariants $\ell_{\min}$ and $\ell_{\max}$ cannot take arbitrary values. For instance, in purely chiral models, they are constrained by the inequality $1/\nu \leq \ell_{\min} \leq \ell_{\max}$.

The simplest examples of such lattice construction appear in the case of dimension $N=1$. For one-dimensional lattices, there is only one independent invariant $\ell_{\max} = \ell_{\min} = \Delta_\Gamma = m$, where m is an odd integer. This number is nothing but the statistical phase of an electron, therefore $Q = 1/\sqrt{m}$ and the filling factor $\nu = 1/m$. Moreover, it is easy to see that the level $l = \Delta_\Gamma/d_H = 1$, hence the charge parameter $\lambda = 1$, and we find that the minimal electric charge is $e^* = 1/m$. We conclude that the QH lattices

$$\Gamma_m = \{n\sqrt{m}\,\mathbf{e} \,|\, n \in \mathbb{Z}\} \tag{E8}$$

with coupling $\mathbf{Q}_m = \mathbf{e}/\sqrt{m}$ and $\nu = 1/m$ are the only ones allowed for $N=1$.

For the two-field case, $N=2$, the construction of allowed lattices is more complex. From the definition of relative angular momenta it follows that we may choose electronic bases with a Gram matrix of the following form:

$$K = \begin{pmatrix} \ell_{\min} & b \\ b & \ell_{\max} \end{pmatrix}. \tag{E9}$$

We consider lattices with $\ell_{\max} < 7$, which are physically most relevant.[43] Then one may simply list all models by going through all possible values of $\ell_{\max}$, $\ell_{\min}$, and b.[8] Furthermore, we limit our attention to the case $\ell_{\min} = \ell_{\max}$, which is most important in the context of our paper.

For convenience, we choose coordinates such that $\mathbf{Q} = (\sqrt{\nu}, 0)$. The condition of unit charge, $\langle \mathbf{Q}, \mathbf{q}_\alpha \rangle = 1$, for $\alpha = 1, 2$, partially fixes the form of electron vectors, $\mathbf{q}_\alpha$, in these coordinates. Namely, $\mathbf{q}_1 = (1/\sqrt{\nu}, s)$ and $\mathbf{q}_2 = (1/\sqrt{\nu}, -s)$, where the number s is yet to be determined. It follows from the requirement $|\mathbf{q}_1|^2 = |\mathbf{q}_2|^2 = \ell_{\max}$ that $s^2 = \ell_{\max} - 1/\nu$. The mutual statistical phase of two electrons, $\theta_{12} = \pi(1/\nu - s^2)$, should be an integer. This implies that $\ell_{\max} + \theta_{12}/\pi = 2/\nu$ is an integer number. Thus we see that the special case $\ell_{\min} = \ell_{\max}$ corresponds to $\nu = 2/m$, where m is an integer. Note that, for $\ell_{\max} < 7$, the converse statement is also true, i.e., for $\nu = 2/m$, *all* the two-dimensional lattices have $\ell_{\min} = \ell_{\max}$.

After some elementary calculations, we find that, for $\nu = 2/m$, Gram matrix (E9) may be expressed as

$$K = \begin{pmatrix} \ell_{\max} & \ell_{\max} - l \\ \ell_{\max} - l & \ell_{\max} \end{pmatrix}. \tag{E10}$$

From condition (32), applied to Eq. (E10), we find that the level $l = 2\ell_{\max} - m = 2s^2$. Therefore, all the lattices in the case $\nu = 2/m$ can be parameterized by *only two* numbers, m and l. It is important to observe that, for all these lattices, $\lambda = 1$. Hence, for two-field models with $\nu = 2/m$, the minimal charge is always $e^* = 1/m$. Introducing a pair of orthogonal vectors, $\mathbf{e}_{1,2}$, so that $\mathbf{q}_{1,2} = \sqrt{m/2}\,\mathbf{e}_1 \pm \sqrt{l/2}\,\mathbf{e}_2$, the lattices may be written explicitly as

$$\Gamma_{ml} = \{\sqrt{m/2}(n_1 + n_2)\mathbf{e}_1 + \sqrt{l/2}(n_1 - n_2)\mathbf{e}_2 \,|\, n_{1,2} \in \mathbb{Z}\}, \tag{E11}$$

and the couplings $\mathbf{Q}_{ml} = \sqrt{2/m}\,\mathbf{e}_1$. Finally, we stress that K matrices (51) and (52) proposed in Sec. IV are exactly the Gram matrices (E10) for the particular case $\nu = 2/3$.

---

[1] *The Quantum Hall Effect*, edited by R. E. Prange and S. M. Girvin (Springer, New York, 1987).

[2] S. Datta, *Electronic Transport in Mesoscopic Systems* (Cambridge University Press, Cambridge, 1999).

[3] G. 't Hooft, *Dimensional Reduction in Quantum Gravity*, in Proceedings of the Salamfest, edited by A. Aly, J. Ellis, and S. Randjbar-Daemi (World Scientific, Singapore, 1993), pp. 284–296; L. Susskind, J. Math. Phys. **36**, 6377 (1995).

[4] The well known examples of the holographic principle in mathematical physics are described in the papers of E. Witten, Adv. Theor. Math. Phys. **2**, 253 (1998); O. Aharony, S. S. Gubser, J. M. Maldacena, H. Ooguri, and Y. Oz, Phys. Rep. **323**, 183

(2000).

[5] Examples of the anomaly inflow at the edge in some other physical systems are provided by J. A. Harvey and O. Ruchayskiy, J. High Energy Phys. (2001) 044; A. Boyarsky, O. Ruchayskiy, and M. Shaposhnikov, Phys. Rev. D **72**, 085011 (2005).

[6] X.-G. Wen, Phys. Rev. B **41**, 12838 (1990).

[7] J. Fröhlich and A. Zee, Nucl. Phys. B **364**, 517 (1991); J. Fröhlich and T. Kerler, *ibid.* **354**, 369 (1991).

[8] J. Fröhlich, U. M. Studer, and E. Thiran, J. Stat. Phys. **86**, 821 (1997).

[9] J. Fröhlich, B. Pedrini, C. Schweigert, and J. Walcher, J. Stat. Phys. **103**, 527 (2001).

[10] X.-G. Wen, Phys. Rev. B **44**, 5708 (1991).

[11] A. M. Chang, L. N. Pfeiffer, and K. W. West, Phys. Rev. Lett. **77**, 2538 (1996).

[12] M. Grayson, D. C. Tsui, L. N. Pfeiffer, K. W. West, and A. M. Chang, Phys. Rev. Lett. **80**, 1062 (1998).

[13] For a review, see A. M. Chang, Rev. Mod. Phys. **75**, 1449 (2003).

[14] D. B. Chklovskii, B. I. Shklovskii, and L. I. Glazman, Phys. Rev. B **46**, 4026 (1992).

[15] C. L. Kane, M. P. A. Fisher, and J. Polchinski, Phys. Rev. Lett. **72**, 4129 (1994); C. L. Kane and Matthew P. A. Fisher, Phys. Rev. B **51**, 13449 (1995).

[16] S. Khlebnikov, Phys. Rev. B **73**, 045331 (2006).

[17] C. L. Kane and Matthew P. A. Fisher, Phys. Rev. Lett. **72**, 724 (1994).

[18] L. Saminadayar, D. C. Glattli, Y. Jin, and B. Etienne, Phys. Rev. Lett. **79**, 2526 (1997); R. de-Picciotto, Nature (London) **389**, 162 (1997).

[19] M. Dolev, M. Heiblum, V. Umansky, A. Stern, and D. Mahalu, Nature (London) **452**, 829 (2008).

[20] F. E. Camino, W. Zhou, and V. J. Goldman, Phys. Rev. Lett. **95**, 246802 (2005).

[21] Y. Ji, Y. Chung, D. Sprinzak, M. Heiblum, D. Mahalu, and H. Shtrikman, Nature (London) **422**, 415 (2003).

[22] R. Guyon, P. Devillard, T. Martin, and I. Safi, Phys. Rev. B **65**, 153304 (2002).

[23] C. L. Kane, Phys. Rev. Lett. **90**, 226802 (2003).

[24] K. T. Law, D. E. Feldman, and Y. Gefen, Phys. Rev. B **74**, 045319 (2006).

[25] E.-A. Kim, M. J. Lawler, S. Vishveshwara, and E. Fradkin, Phys. Rev. B **74**, 155324 (2006).

[26] V. V. Ponomarenko and D. V. Averin, Phys. Rev. Lett. **99**, 066803 (2007).

[27] I. Neder, M. Heiblum, Y. Levinson, D. Mahalu, and V. Umansky, Phys. Rev. Lett. **96**, 016804 (2006); I. Neder, F. Marquardt, M. Heiblum, D. Mahalu, and V. Umansky, Nat. Phys. **3**, 534 (2007).

[28] E. Bieri, Ph.D. thesis, University of Basel, 2007; E. Bieri, M. Weiss, O. Göktas, M. Hauser, C. Schönenberger, and S. Oberholzer, Phys. Rev. B **79**, 245324 (2009).

[29] P. Roulleau, F. Portier, D. C. Glattli, P. Roche, A. Cavanna, G. Faini, U. Gennser, and D. Mailly, Phys. Rev. B **76**, 161309(R) (2007); Phys. Rev. Lett. **100**, 126802 (2008).

[30] L. V. Litvin, H.-P. Tranitz, W. Wegscheider, and C. Strunk, Phys. Rev. B **75**, 033315 (2007); L. V. Litvin, A. Helzel, H.-P. Tranitz, W. Wegscheider, and C. Strunk, *ibid.* **78**, 075303 (2008).

[31] E. V. Sukhorukov and V. V. Cheianov, Phys. Rev. Lett. **99**, 156801 (2007).

[32] J. T. Chalker, Y. Gefen, and M. Y. Veillette, Phys. Rev. B **76**, 085320 (2007).

[33] I. Neder and E. Ginossar, Phys. Rev. Lett. **100**, 196806 (2008).

[34] S.-C. Youn, H.-W. Lee, and H.-S. Sim, Phys. Rev. Lett. **100**, 196807 (2008).

[35] I. P. Levkivskyi and E. V. Sukhorukov, Phys. Rev. B **78**, 045322 (2008).

[36] We define the statistical phase θ_{12} of two operators ψ_1 and ψ_2 via the relation $\psi_1(x)\psi_2(x')=e^{i\theta_{12}}\psi_2(x')\psi_1(x)$. The microscopic construction (Ref. 59) shows that so defined statistical phase indeed takes integer values for single valued excitations of the Laughlin state (Ref. 40).

[37] S. B. Treiman, R. Jackiw, and D. J. Gross, *Lectures on Current Algebra and its Applications* (Princeton University Press, Princeton, NJ, 1972).

[38] X.-G. Wen, *Quantum Field Theory of Many-body Systems* (Oxford University Press, New York, 2007).

[39] A. O. Gogolin, A. A. Nersesyan, and A. M. Tsvelik, *Bosonization and Strongly Correlated Systems* (Cambridge University Press, Cambridge, 1998).

[40] R. B. Laughlin, Phys. Rev. Lett. **50**, 1395 (1983).

[41] In fact, the introduced matrix $q_{\alpha i}$ is an analog of the well known Cabibbo-Kobayashi-Maskawa matrix in particle physics.

[42] Note that introducing new fields $\chi_\alpha = \Sigma_i q_{\alpha i}\phi_i$, one arrives at the action $S=\int dt dx[K^{-1}_{\alpha\beta}\partial_t\chi_\alpha\partial_x\chi_\beta + V_{\alpha\beta}\partial_x\chi_\alpha\partial_x\chi_\beta]$, which is often used in the literature. However, this form of the action is not convenient for the classification of effective models and may lead to a number of confusions.

[43] Numerical simulations (Ref. 60) show that for larger values of statistical phases the QH state is not stable and electrons form a Wigner crystal (Ref. 1).

[44] X. G. Wen, Phys. Rev. Lett. **64**, 2206 (1990); A. H. MacDonald, *ibid.* **64**, 220 (1990); M. D. Johnson and A. H. MacDonald, *ibid.* **67**, 2060 (1991).

[45] J. K. Jain, Phys. Rev. Lett. **63**, 199 (1989).

[46] Z.-X. Hu, H. Chen, K. Yang, E. H. Rezayi, and X. Wan, Phys. Rev. B **78**, 235315 (2008).

[47] R. G. Clark, S. R. Haynes, J. V. Branch, A. M. Suckling, P. A. Wright, P. M. W. Oswald, J. J. Harris, and C. T. Foxon, Surf. Sci. **229**, 25 (1990); J. P. Eisenstein, H. L. Stormer, L. N. Pfeiffer, and K. W. West, Phys. Rev. B **41**, 7910 (1990); L. W. Engel, S. W. Hwang, T. Sajoto, D. C. Tsui, and M. Shayegan, *ibid.* **45**, 3418 (1992).

[48] We assume that both QPCs are either in a weak tunneling regime or in a weak backscattering regime. Moreover, we further assume that two channels at each QH edge originate from the same Ohmic contact, and therefore, they are equally biased.

[49] M. Marino, *Chern-Simons Theory, Matrix Models, and Topological Strings* (Oxford University Press, Oxford, 2005).

[50] Expression (C5) implies that, strictly speaking, the amplitudes t_ℓ in tunneling Hamiltonian (C1) contain Wilson lines that connect tunneling point at opposite edges in the left and right QPCs. They have to be taken into account when evaluating the overall AB phase shift in the tunneling amplitudes [Eq. (59)].

[51] Claudio de C. Chamon and Eduardo Fradkin, Phys. Rev. B **56**, 2012 (1997).

[52] A. Stern, Ann. Phys. **323**, 204 (2008).

[53] D. E. Feldman and A. Kitaev, Phys. Rev. Lett. **97**, 186803 (2006); D. E. Feldman, Y. Gefen, A. Kitaev, K. T. Law, and A. Stern, Phys. Rev. B **76**, 085333 (2007).

[54] D. J. Thouless and Y. Gefen, Phys. Rev. Lett. **66**, 806 (1991).

[55] J. Fröhlich and B. Pedrini, in *Statistical Field Theories* (Kluwer Academic Publishers, Dordrecht, 2002).

[56] Topological defects (vortices) of the b field, if present in the bulk, change the relation between fields $b_{\mu i}$ and A_μ. Note, however, that these defects cost a large energy (see also the discussion in Appendix C). Therefore, we do not consider them.

[57] It is important that at the edge $\partial_\mu j_i^\mu \neq 0$, therefore the charge density is not determined by the b field. In other words the edge deformation does not generate the topological reconstruction in the bulk and leads only to the accumulation of the charge.

[58] J. Fröhlich and E. Thiran, J. Stat. Phys. **76**, 209 (1994).

[59] A. Boyarsky, V. V. Cheianov, and O. Ruchayskiy, Phys. Rev. B **70**, 235309 (2004).

[60] X. Zhu and Steven G. Louie, Phys. Rev. B **52**, 5863 (1995).